UNIVERSITY OF GENOA

POLYTECHNIC SCHOOL

Department of Civil, Chemical and Environmental Engineering

MASTER'S DEGREE COURSE IN

CHEMICAL AND PROCESS ENGINEERING

Brushite-based bone cements as drug carriers: synthesis and characterization

Supervisors:

Prof. Elisabetta Finocchio

Prof. Alberto Lagazzo

Co supervisor:

Prof. Pier Francesco Ferrari

Candidate:

Giulia Peluffo

Academic year 2023-2024

General index

Abstract 5

1. Introduction 6

1.1 Bones and their structure 6

1.2 Bone tissue 6

1.3 Types of bones 8

1.4 Bone diseases and treatments 9

1.5 Bone cements 10

1.5.1 Brushite-based bone cements 14

1.6 Bone cements and chemical retardants 15

1.7 Bone cements and drugs 16

2. Materials and methods 17

2.1 Preparation 18

2.2 Ibuprofen, naproxen and gentamicin 20

2.3 Characterization 23

2.3.1 Theory of the FT-IR 25

2.3.2 Practical application of FT-IR 27

2.3.3 TGA 29

2.3.4 DSC 31

2.3.5 Drug release 32

3. Results and discussion 36

3.1 Sample workability 36

3.2 FT-IR Spectra 37

3.3 Thermal evolution 48

3.4 Study of ibuprofen release 61

4. Conclusions 64

5. Acknowledgements 66

6. References 67

Figure index

Figure 1. Bone anatomy. 7
Figure 2. Types of bones 8
Figure 3. Possible improved approaches for calcium phosphate cements 12
Figure 4. Injectability properties. 13
Figure 5. Example of some samples made in the laboratory. 18
Figure 6. Example of sample extrusion. 19
Figure 7. Structure of ibuprofen sodium salt. 21
Figure 8. Structure of naproxen sodium. 22
Figure 9. General structure of gentamicin. 22
Figure 10. Thermo Nicolet 380 Nexus FT-IR spectrometer. 25
Figure 11. FT-IR scheme. 27
Figure 12. Examples of tablets. 28
Figure 13. Scheme of home-made instrument. 29
Figure 14. STA Netzsch 409 thermobalance. 31
Figure 15. Netzsch DSC 300 Caliris 32
Figure 16. Nanoquant plate 33
Figure 17. Tecan Spark. 34
Figure 18. Robbins Scientific Rotary Blood Mixer / Agitator. 35
Figure 19. FT-IR Spectra od brushite 2:1 and 3:1 (common scale). 37
Figure 20. FT-IR Spectra of brushite 2:1 and 3:1, brushite 3:1 + retardant 0.5 M and 1 M (no common scale)…… 40
Figure 21. FT-IR Spectra of ibuprofen, brushite 2:1, brushite 2:1 + ibuprofen 10% and 20% (no common scale)……..…….41
Figure 22. FT-IR Subtraction spectra of brushite 2:1 + ibuprofen 20% and ibuprofen. ……...43
Figure 23. FT-IR Spectra of brushite 2:1, brushite 2:1 + naproxen 10% and naproxen (no common scale)…….…….. 45
Figure 24. FT-IR Subtraction spectra of brushite 2:1 + naproxen 10% and brushite 2:1. …….……..…….46
Figure 25. FT-IR Spectrum of gentamicin. 47
Figure 26. FT-IR Spectrum of brushite 2:1 + gentamicin 3%. 48
Figure 27. TGA brushite 2:1. ..... …..49
Figure 28. FT-IR brushite 2:1 at different temperatures increasing from the bottom (no common scale)……...50
Figure 29. TGA brushite 2:1 + ibuprofen 20%. 50
Figure 30. TGA ibuprofen. 51
Figure 31. FT-IR brushite 2:1 + ibuprofen 20% at different temperatures increasing from the bottom (no common scale)……..52
Figure 32. TGA brushite 2:1 + naproxen 10%. 53
Figure 33. TGA naproxen. 54
Figure 34. FT-IR Spectra of brushite 2:1, brushite 2:1 + ibuprofen 20% and brushite 2:1 + naproxen 10% after TGA (no common scale)…….55
Figure 35. TGA brushite 2:1 + gentamicin 3%. 56
Figure 36. TGA gentamicin. 57
Figure 37. DSC of brushite 2:1, brushite 2:1 + ibuprofen 20% and brushite + naproxen 10% 58

Figure 38. DSC ibuprofen..... 59
Figure 39. DSC naproxen. 60
Figure 40. DSC brushite 2:1 + gentamicin 3%. 61
Figure 41. Calibration curve before freezing. 62
Figure 42. Calibration curve of ibuprofen after freezing (5 days). 62
Figure 43. Calibration curve of ibuprofen after freezing (9 days). 63
Figure 44. Ibuprofen release in time. Where B+I =brushite 2:1 + ibuprofen 20%, B=brushite 2:1 and PBS……63

Table index

Table 1. Samples. 20
Table 2. Summary of analysis made on the samples. 24
Table 3. References. 35
Table 4. Experimental data of IR brushite. 39

Abstract

Bone cements are biomaterials used for bone regeneration when natural bone regeneration is insufficient. They are biocompatible and have the mineral component similar to that of bone. These materials have been used for several years in dental and orthopedic fields but ongoing studies aim to expand their possible applications. In fact, they could be used as drug carriers and also in the treatment of various diseases that compromise the skeletal system.

There are several types of bone cements, including brushite-based cements ($CaHPO_4 \cdot 2(H_2O)$) that can be molded and inject.

In this research, samples of brushite-based bone cements were synthesized and loaded with two anti-inflammatory agents (ibuprofen and naproxen) and one antibiotic (gentamicin). The effects as setting retardants for each were also studied. Three techniques were used to analyze the various samples: infrared spectroscopy attenuated total reflectance (IR ATR) and Fourier transform infrared spectroscopy in transmittance mode (FT-IR) with both powder and tablet material, thermogravimetric analysis (TGA) and differential scanning calorimetry (DSC). In the case of ibuprofen, release tests were executed to get a better understanding of how it changes over time.

1. Introduction

1.1 Bones and their structure

The human body has 206 bones and the skeletal system acts as a rigid support for the other organs, while, together with muscles and joints, ensures the ability to move. In addition, it has the function of producing blood cells, mineral storage and endocrine regulation. In fact, the internal cavities contain the bone marrow, the site of maturation for the progenitor cells that form the blood elements.

The skeletal system must endure physical stresses that predispose it to injury. In recent years, several studies have focused on the development of materials that contain the elements found in bones and also enriched with drugs such as bone cements [1].

1.2 Bone tissue

Bone tissue is part of the supporting connective tissues. It has the function of locomotion, support, protection of soft tissue and harboring of bone marrow. This tissue is rich in mineral salts such as calcium and phosphorus. It is composed of 10% water by weight and 90% mineralized extracellular matrix [2]. The organic part of the matrix contains collagen proteins (90%), mainly type I and other proteins. The inorganic one contains is mainly phosphate and calcium ions but also magnesium, bicarbonate, sodium, potassium, zinc, fluorite and other minerals. Phosphate and calcium ions form the crystals of hydroxyapatite ($Ca_{10}(PO_4)_6(OH)_2$), which together with collagen proteins form a scaffold for hydroxyapatite deposition that provides strength and rigidity [3].

Bones are lined by the periosteum, a dense, vascularized connective tissue, while the interior is lined by the endosteum.

Bone tissue contains four types of cells (**Figure 1**):

1. Osteoblasts, which produce the extracellular matrix and regulate its mineralization. When they change to less active cells they become osteocytes.
2. Osteocytes, that occupy bone gaps, communicating with each other via extensions.

3. Osteoclasts, large and multinucleated, that take up extracellular matrix in remodeling processes. They have lysosomes with enzymes that can digest organic components of the matrix.
4. Osteoprogenitor cells, derived from stem cells and that can transform into osteoblasts [2].

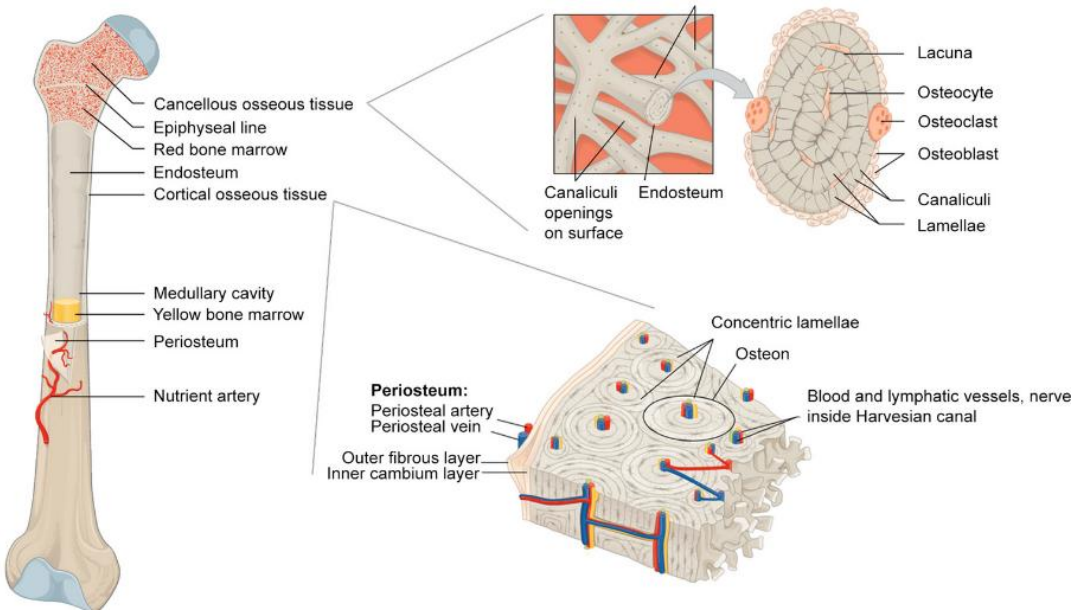

Figure 1. *Bone anatomy [1].*

Cells continuously remodel bone and are known to communicate with each other during this process. In fact, the interaction between osteoblasts and osteoclasts ensure the coupling from bone resorption to bone formation. Bone remodeling is under the control of several factors that contribute to bone homeostasis. During this process, old bone is replaced by new bone following 3 stages:

1. Osteoclasts begin to resorb bone.
2. Transition period.
3. Osteoblasts form new bone.

Remodeling is necessary, for example, to heal from fractures and for calcium homeostasis [3].

There are two types of bone tissue: lamellar and non-lamellar. The former can be compact or spongy type [2].

1.3 Types of bones

The skeleton consists of 206 bones, each with different characteristics. They are classified into (**Figure 2**):

1. Long bones, that have an elongated body or diaphysis (containing the medullary cavity with the bone marrow) with two enlarged ends or epiphyses.
2. Short bones, which have a core of spongy bone tissue surrounded by compact bone tissue.
3. Flat bones, which consist of a layer of spongy bone tissue covered by compact layered bone tissue.
4. Sesamoid bones, that develop in the thickness of some ligaments and tendons near articular surfaces.
5. Irregular bones, which have shapes that do not fit into any of the other categories [2].

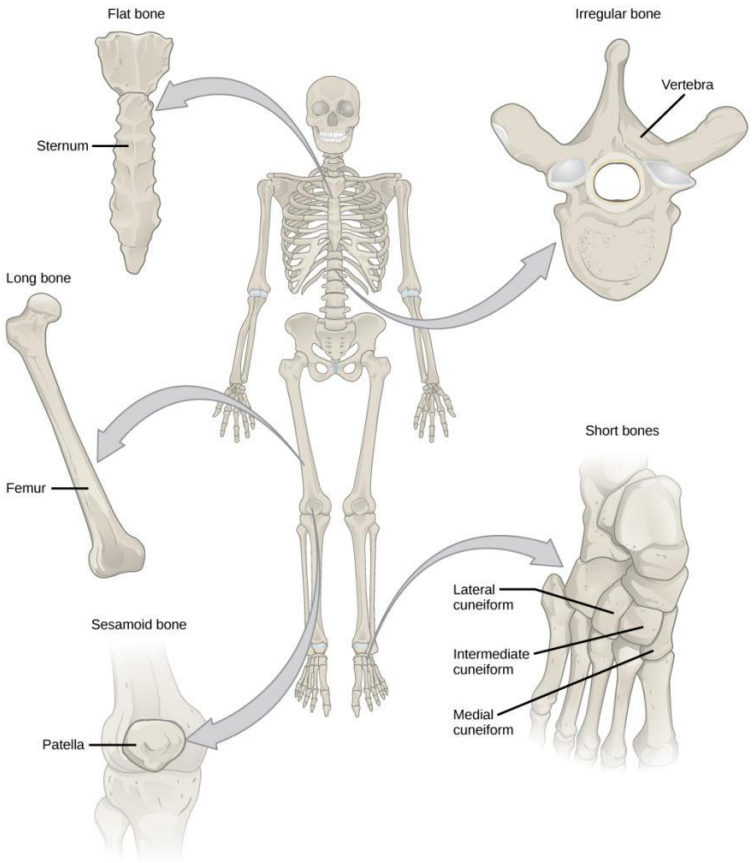

Figure 2. *Types of bones [4].*

1.4 Bone diseases and treatments

Various pathologies affect the skeletal system, particularly bone tissue. They can be caused by imbalance between bone resorption and formation. Some pathologies include the following:

- Osteoporosis, that is characterized by decrease in bone mass and mineral density.
- Paget's disease, which affects the bone remodeling process.
- Osteogenesis imperfecta, that causes the bones to fracture easily.
- Bone tumors and cancers [5].

In the former case, if osteoclasts excessively resorb bone tissue without the corresponding amount of newly formed bone by osteoblasts it contributes to bone loss and osteoporosis (the opposite is osteopetrosis). Estrogen also plays a crucial role in bone tissue homeostasis; its decrease in menopause is the main cause of bone loss and osteoporosis [3].

The conditions mentioned above compromise bone strength and density and consequently increase the risk of fractures from even minor trauma. In recent years, various biomedical and engineering research has been done to develop materials that can ensure proper bone regeneration if natural bone regeneration is insufficient. These include bone cements, one of the fields in which more experimental research has been carried out. They can also be combined with specific drugs to have dual action.

For example, the effect of conventional treatments for bone metastases is still limited. Therefore, more recent studies have focused on finding materials that can carry drugs to have a targeted action. One such material is hydroxyapatite, that is used as bone cement and is biocompatible [6]. Several *in vitro* experiments have shown that calcium phosphate-based drug-containing bone cements suppress the proliferation of cancer cells. Moreover, when they are incorporated in high concentrations, they are able to kill cancer cells [7].

Another case concerns the treatment of osteoporosis using zoledronic acid (ZA). However, it causes several side effects such as renal toxicity and hypocalcemia so a controlled delivery system using calcium phosphate (CaP) has been considered. This bone graft carrier is biocompatible and has been used as a biomaterial for bone grafts since it is crucial in bone regeneration. Studies done have shown that the combination of the two components can give long-term benefits when used in the correct doses.

The results also suggest that they might help inhibit excessive bone formation during the treatment of metastatic bone cancer [8].

1.5 Bone cements

Bone graft materials can be classified into autografts, allografts and xenografts. They may have some downsides in terms of infection and immune responses once implanted. Therefore, materials with characteristics similar to the composition of bone have been studied: bone cements. These materials generally consist of a mixture of powders and a liquid, often water. The setting process is achieved by a chemical polymerization reaction, this produces a paste that can also be used in the medical field [9].

They were developed in the 1940s and 1950s with the first uses in dentistry and orthopedics but over the years they have been studied to expand their use, especially as drug carriers. Bone cements are biomaterials used for bone regeneration when natural bone regeneration is insufficient. Their special feature is that these cements are biocompatible and have the mineral component similar to that of bone. An important aspect that should be considered is that the polymerization reaction generated during the formation of bone cements is exothermic and relatively fast-setting. Therefore, chemical setting retardants are often used. Even in the case of drugs that can be combined, the exothermicity of the reaction should be considered, also any properties as setting retardants should be studied [10].

The cements must satisfy the required properties such as precise setting time and rheology similar to bone tissue, they must have anti-washout properties when coming into contact with body fluids. Bone cements must be sufficiently cohesive, otherwise particles can enter the bloodstream with serious consequences such as thrombus vascular blockage and pulmonary embolism. Then disintegrated particles can result in inflammatory response. Therefore, all samples must first be thoroughly studied and analyzed [9].

The performance of bone cement scaffolds created by engineering bone tissue engineering (BTE) also depends on properties such as:

- Biocompatibility, this avoids the immune and inflammatory response, the scaffolds must be nontoxic.

- Bioactivity, which is inherent or supplemented by the addition of biological actives. Bioactivity enhances osteogenesis, vasculogenesis, and angiogenesis.
- Protein adsorption.
- Osteoconductivity and osteoinductivity. The former enables adhesion, proliferation, biomineralization, and deposition of bone cells, and the latter enhances new bone formation.
- Bioactive fixation, which is the ability of the active surfaces to create a chemical bond with the bone, thereby reducing the formation of the fibrous capsule.
- Resorption, scaffold degradation should be controlled to be properly replaced with new bone formation.
- Sterilization, that is important to avoid infection and cause rejection. Various methods can be used such as autoclaving, dry heat, ethylene oxide gas sterilization, and gamma or electron beam irradiation.

Further aspects of the scaffolds are the mechanical ones:

- Crystallinity, this characteristic influences the solubility and biosorption of materials *in vivo*.
- Porosity, since the size, shape and distribution of pores determines the function of the scaffold.
- Wettability, which is measured by the water uptake ratio of the scaffold, that influences the oxygen and nutrient transport inside. It can be evaluated by contact angle measurement.
- Roughness (topography) [11].

A property that bone cements lack is antibacterial one. In fact, these materials present a risk of post-operative infection. To address this deficiency, it is crucial to combine elements such as silver ions (Ag^+) or silver nanoparticles (AgNPs), or a variety of drugs [12].

Nowadays there are several types of bone cements, with different biomechanical properties. The first and commonly used bone cement is polymethylmethacrylate (PMMA) acrylic cement ($(C_5O_2H_8)_n$). PMMA is one of the most versatile materials and plays a key role in orthopedics, spinal and tumor surgery [10]. One disadvantage of this bone cement is that PMMA does not degrade in the human body and often must be removed by surgery [12].

Another bone cement with chemical and biological characteristics similar to the bone mineral phase are calcium phosphates (CaP). For the solid phase, one or more calcium phosphate compounds are used. For the liquid

one, water or a solution containing calcium or phosphate is used and may also contain chitosan, alginate, hyaluronate, gelatin or citric acid. These bone cements have different formulations but there are two possible end products: brushite (dicalcium phosphate dihydrate, DCPD) or apatite, such as like hydroxyapatite or calcium-deficient hydroxyapatite. The former is more soluble than the latter [13].

CPCs (CaP bone cements) are used by implanting grafts in the form of blocks or granules, so the shape and size of the bone defect must be known previously. The paste these materials form is moldable and can self-set *in vivo*, this brings medical benefits in the treatment of fractures related to osteoporosis or other bone defects. CPCs also have very rapid setting times that should be taken into consideration if they are to be used in a medical operation [14]. These cements have excellent bioactivity but year slow degradation, so they need to be improved with additives to control it [15].

However, scaffolds are not always adaptable to the site on the bone, so injectable bone cements have also been studied and made. There are several possibilities to improve these materials since they exhibit poor degradability, lack of macroporosity, and weak mechanical properties (**Figure 3**) [9].

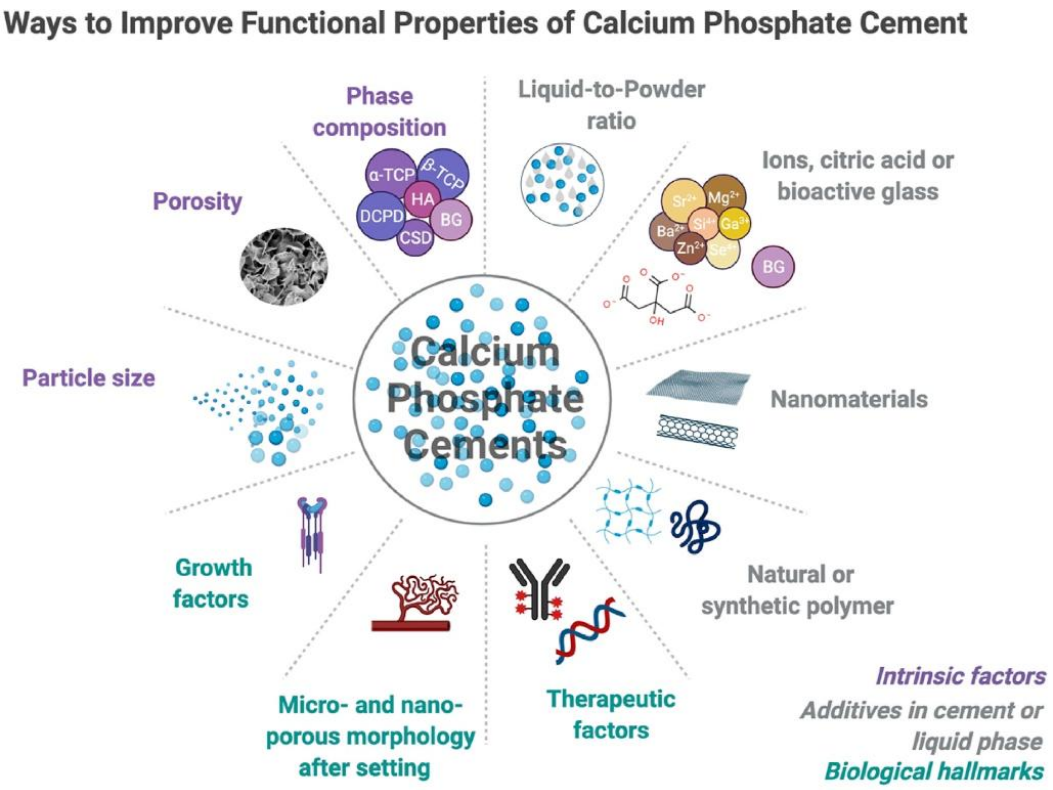

Figure 3. *Possible improved approaches for calcium phosphate cements [9].*

Various formulations of phosphate cements are available for clinical trials but these have also disadvantages, including the potential for pathogenic bacterial attachment after implantation. Therefore, in both of the examples above, it is essential to combine them with drugs that can prevent complications [12]. The low setting temperature of CPCs makes them ideal for such combinations or for use with bioactive molecules that enhance the bone regeneration capacity of these cements. Additionally, their porosity contributes to their suitability for this purpose. Key factors to consider include the amount of liquid phase, the ratio of components, the particle size and the presence of retardants. All these factors brings changes in structure, setting time and other properties [16].

Another important property relating to these materials is injectability. It can be defined as the ability of a paste to extrude through the syringe. The extruded paste must keep its homogeneity (**Figure 4**) [9].

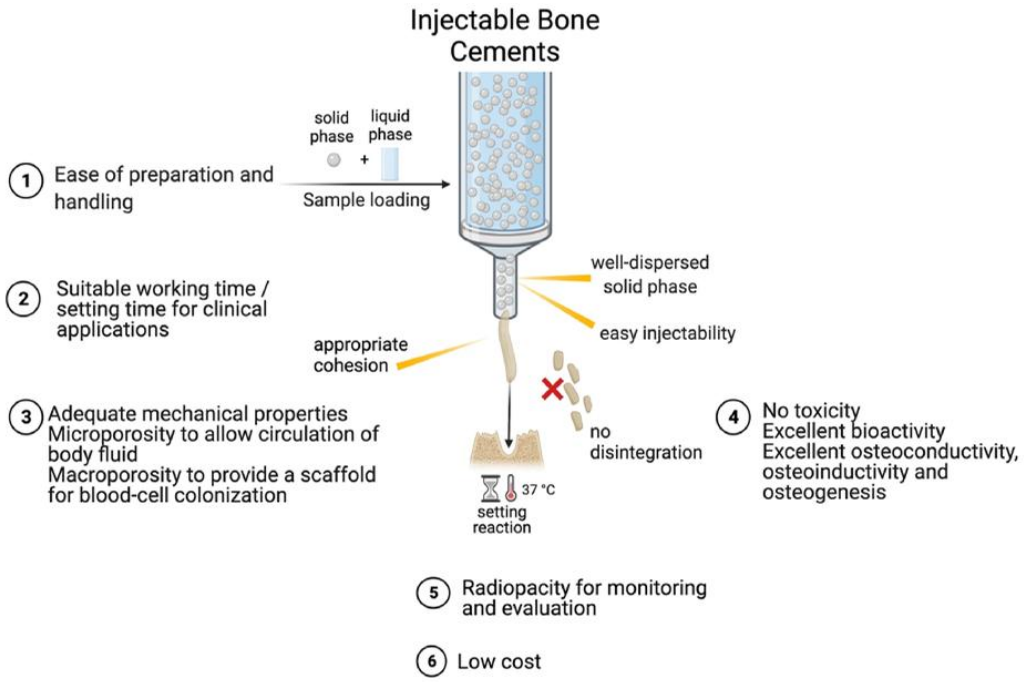

Figure 4. *Injectability properties [9].*

For these materials, pH must also be taken into consideration. In fact, to minimize cell death of those and incorporated in the cement, it is necessary to have cement formulations with setting reactions close to physiological pH or additives can be included to regulate it [17].

Bone cement scaffolds can also be made with a 3D printer. This technology is based on the principle of layering and is suitable for mimicking porous

bone structure. By using these scaffolds, cells seeded *in vitro* with possible drugs can be transplanted directly into the bone site. The ideal material should to simulate the biological functions of bone composition and provide a temporary site for proliferation of cells and blood vessels [17]. So these scaffolds are made of biocompatible materials such as ceramics, polymers or a combination of them. The proper choice of material depends on several factors such as biodegradability, strength, and ability to facilitate cell adhesion and growth [18]. Currently, these materials have high strength but poor surface properties and low plasticity. These scaffolds have already been used but also have other limitations such as poor osteogenic properties resulting in slow healing. The latter is also affected by the size of the bone defect. Some defects are difficult to repair because of the internal growth of fibrous connective tissue [17]. Scaffolds made with a 3D printer must be sterile and compatible with the implant site. They are an excellent option for custom bone repair [18].

1.5.1 Brushite-based bone cements

The bone cement on which this research has focused on is brushite ($CaHPO_4 \cdot 2(H_2O)$) that can be molded and injected. It is part of the CPCs and is a type of hydrated calcium phosphate. From the brushite formation reaction, a paste is obtained that sets in a short time, which is why setting retardants should be used. This reaction consume a significant amount of water [19]. Brushite is a metastable phase that can transform into apatite [13].

Brushite-forming calcium phosphate bone cements are biocompatible and bioresorbable, they present osteoconductivity, self-setting and injectability characteristics. However these cements have low mechanical strength. Brushite is degraded by chemical dissolution [20] and when implanted in the human body it promotes bone bonding and over time is replaced by new tissue [19]. Several properties including setting time and rate of resorption must be regulated to successfully achieve clinical application. The self-setting of the brushite must allow the surgeon to operate in the correct manner and therefore the ideal setting time would be in the range of a few minutes. The injectability of the paste should also be checked if minimal-invasive operations are involved, since it is directly inserted through a syringe with narrow cannulas. To improve this property, particle size can be adjusted, also using additives such as citric acid. Rheological properties should also be considered. These cements are considered viscoelastic since

they change from mainly liquid properties immediately after mixing to mainly solid properties after curing. The mechanical properties are also crucial since a compressive strength close to 10-12 MPa comparable to that of trabecular bone is required. Therefore, the characteristics of the initial powders, the hydrated phases formed and the liquid-to-powder ratio must be studied [20].

There are several studies involving ion-doped brushite or as a potential carrier of drugs such as ibuprofen and gentamicin, on which this research is based.

1.6 Bone cements and chemical retardants

Setting retardants can be added to the mixture used to create a bone cement to make it more workable and to adjust the setting time. The retardant acts by slowing down the chemical reaction. Two possible methodologies are to take advantage of the chelation effect and coatings, or one can use smaller particle size or adjust the ratio of powders to liquid. The pH of the paste formed is a parameter that should be considered and kept under control even when retardants are added.

Some retardants also help to achieve greater strength of the final product, such as:

- The incorporation of 10% by weight of calcium carbonate ($CaCO_3$).
- SO_4^{2-}.
- α-hydroxyl acids (citric, glycolic, malic and tartaric acids) and their salts (as sodium citrate), which allow easier mixing and processing of cement with a reduced liquid/powder (L/P) ratio (related to reduced porosity), resulting in improved strength.
- Free ions ($Sr^{2+}, Mg^{2+}, Si^{4+}$), which do not always result in strength improvement [13].

Citric acid ($C_6H_8O_7$) also interferes with the crystallization mechanism [21]. Moreover, citrate ions have low toxicity and have been reported to be present in bone. So does sodium citrate ($Na_3C_6H_5O_7$, which was used in this research work) inhibits the crystallization of calcium phosphate, hindering nucleation and crystal growth. As a result, the setting time is slowed. It acts by chelation of calcium, thus limiting the availability of its ions to form the crystal lattice [22]. Both of these two retardants are used

more in brushite cements. Similar effect can be obtained with chondroitin 4-sulfate and glycolic acid ($HOCH_2COOH$) [23].

Two other generic regulators of setting time are sodium pyrophosphate ($Na_2H_2P_2O_7$) and magnesium sulfate ($MgSO_4$), the amount of which should be adjusted to take advantage of their action as retardants [22].

For dental applications, borax (sodium tetraborate decahydrate, $Na_2B_4O_7 \cdot 10H_2O$) is used to adjust the setting time of impression materials [24].

Overall, chemical retardants can also make positive changes on bone cements; they can make the paste more injectable or improve mechanical properties [22].

1.7 Bone cements and drugs

As explained in previous chapters, it is essential to combine bone cements with drugs to make them have antibacterial properties and also to take advantage of their characteristics as setting retardants. The addition of drugs directly at the cement preparation stage allows local targeted delivery of the drug itself into the body [12]. The water solubility of these substances is a key factor to consider to ensure that they come together properly with the cements [19]. This contributes to long-term success in graft operations to avoid possible rejection and other post-operative complications. However, the correct doses must be used to avoid potential side effects [12]. The effects of both certain anti-inflammatory drugs (such as ibuprofen and naproxen) anti-cancer drugs (such as mercaptopurine) and certain antibiotics (such as gentamicin), have been studied. Ibuprofen and gentamicin have been used in this research work.

A bone cement used as a carrier of the drug must incorporate it, hold it at a specific target site, and release it gradually over time into the human body. First, it is necessary to verify that the addition of the drug studied does not interfere in the setting reaction and that it does not negatively change the chemical and physical properties. Next, characterization of the *in vitro* release kinetics must be done and then the efficacy of the bone cement as a vehicle for drug delivery *in vivo* must be evaluated. Drug release depends on several factors: microstructure, solubility of the drug, the type of binding between the drug and the cement matrix, and the degradation mechanism of the matrix itself. For example, CPCs belong to the category of devices with controlled diffusion, in these the drugs can be either mixed with the

liquid phase or introduced either into the powders. The porosity of these materials has a key role in release mechanism. If the release of the antibiotic was too rapid, the researchers opted to incorporate some polymers (for example, sodium alginate or chitosan) into the bone cement to delay the release of the drug.

In the case of anti-inflammatory drugs, experiments have been conducted with aspirin, whose release rate increases with increased porosity of bone cement, and with indomethacin (non-steroidal). In the last case, it was found that its half-life in plasma was much higher when indomethacin was introduced using a cement implant as opposed to subcutaneous injection [25]. As mentioned earlier, ibuprofen (non-steroidal) has also been studied, it is the most widely used to treat bone infections and it is often used with CPCs. It affects the setting reaction of the cement and slows it down, it should be considered that, once implanted, it could affect the body's inflammatory response. This drug also alters the mechanical properties of these materials. Also his encapsulation has been evaluated, especially in poly lactic-co-glycolic acid (PLGA) nanoparticles (NP) to promote a sustained drug release [26].

For apatitic cements, it has been found that antibiotics tend to increase setting times and the effect of flomoxef sodium dissolved in the liquid phase was studied. For other CPCs, also the effect of vancomycin has been studied. Both involved changes in mechanical properties.

In brushite cements, which are more resorbable than apatitic cements, gentamicin sulfate can be used either in powder or solution form. Studies have observed that its addition affects the setting time and increases it. It also increases mechanical strength due to the presence of sulfate ions in the antibiotic [25].

An example of a commercially available bone cement with retarding properties is Cemex® Genta LV produced by Tecres SpA. It is loaded with gentamicin, and its low viscosity allows it to be easily injected during surgical procedures [27].

2. Materials and methods

Methodical preparations were carried out that enabled the completion of the set studies. To accomplish this, different materials were used and certain procedures explained below were done.

2.1 Preparation

In this experiment, brushite (dicalcium phosphate dihydrate) was used as bone cement. It was prepared by mixing water and a mixture of β-Tricalcium phosphate ($Ca_3(PO_4)_2$) and monocalcium phosphate ($Ca(H_2PO_4)_2 \cdot H_2O$), both in powder. This process leads to a moldable paste that solidifies to form brushite, this reaction is exothermic.

The synthesis reaction is as follows [28]:

$$Ca_3(PO_4)_2 + Ca(H_2PO_4)_2 \cdot H_2O + 7H_2O \rightarrow 4CaHPO_4 \cdot 2H_2O$$

Several samples, both inert and bioactive, were prepared during the experiment. The rate at which the components react to form brushite is very rapid so a retardant must be used if the reaction wants to be delayed. Therefore, these samples were loaded with a chemical retardant, sodium citrate ($Na_3C_6H_5O_7$), and with different drugs: ibuprofen sodium salt, naproxen sodium, and gentamicin sulfate. The first two are anti-inflammatory and the last is an antibiotic. The retardant and drugs were added to the aqueous phase. This retardant was also chosen because of previous studies at the laboratory and because of the results obtained from the literature search (**1.6 Bone cements and chemical retardants**). The same applies to the drugs used (**1.7 Bone cements and drugs**).

The samples are cylindrical, approximately 2 cm high and 1 cm of diameter. Of each sample, at least 3 were made (**Figure 5**).

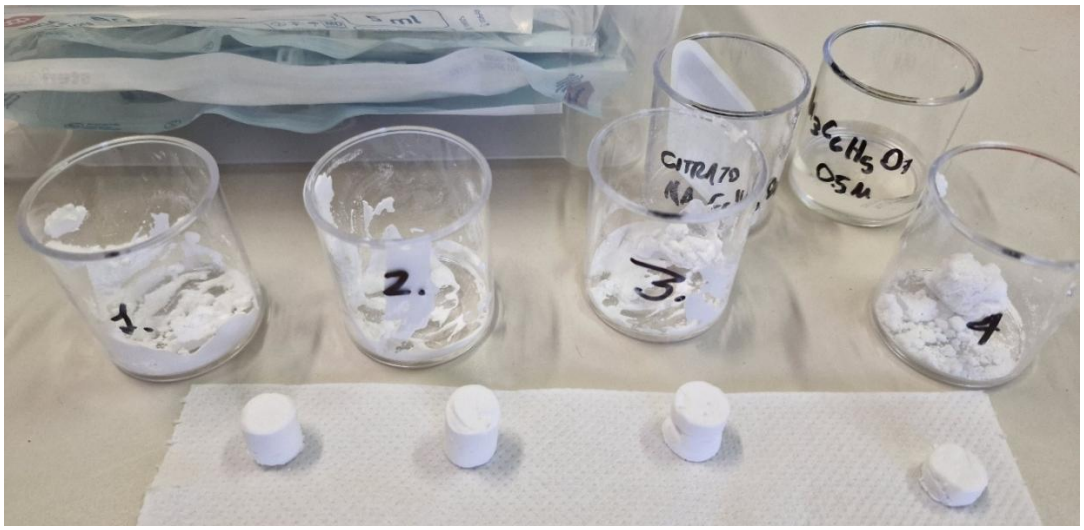

Figure 5. *Example of some samples made in the laboratory.*

These samples were extruded through the use of a cut syringe without a needle (**Figure 6**).

Figure 6. *Example of sample extrusion.*

Table 1 summarizes all the different samples prepared:

Table 1. *Samples.*

Sample	S/L ratio	Amount of β-TCP [g]	Amount of calcium phosphate monohydrate [g]	Amount of distilled water [g]	Retardant: Sodium citrate 0.5M	Retardant: Sodium citrate 1M	Amount of Ibuprofen [%]	Amount of Naproxen [%]	Amount of Gentamicin [%]
1. Stoichiometric brushite	[-]	3.1	2.52	1.26	No	No	[-]	[-]	[-]
2. Brushite 1:1	1:1	3.1	2.52	5.62	No	No	[-]	[-]	[-]
3. Brushite 2:1	2:1	3.1	2.52	2.81	No	No	[-]	[-]	[-]
4. Brushite 3:1	3:1	3.1	2.52	1.87	No	No	[-]	[-]	[-]
5. Stoichiometric Brushite + retardant (0.5M)	1:1	3.1	2.52	1.26	Yes	No	[-]	[-]	[-]
6. Brushite 2:1 + retardant (0.5 M)	2:1	3.1	2.52	2.81	Yes	No	[-]	[-]	[-]
7. Brushite 3:1 + retardant (0.5 M)	3:1	3.1	2.52	1.87	Yes	No	[-]	[-]	[-]
8. Brushite 3:1 + retardant (1 M)	3:1	3.1	2.52	1.87	No	Yes	[-]	[-]	[-]
9. Stoichiometric brushite + retardant (1M)	[-]	3.1	2.52	1.26	No	Yes	[-]	[-]	[-]
10. Brushite 2:1 + Ibuprofen 20%	2:1	3.1	2.52	2.81	No	No	20%	[-]	[-]
11. Brushite 2:1 + Ibuprofen 10%	2:1	3.1	2.52	2.81	No	No	10%	[-]	[-]
12. Brushite 2:1 + Naproxen 10%	2:1	3.1	2.52	2.81	No	No	[-]	10%	[-]
13. Brushite 2:1 + Gentamicin 3%	2:1	3.1	2.52	2.81	No	No	[-]	[-]	3%

The percentage is to be considered w/w.

2.2 Ibuprofen, naproxen and gentamicin

In order to better understand the results obtained, it is useful to consider the chemical structure of the drugs used.

1. Ibuprofen sodium salt (**Figure 7**)

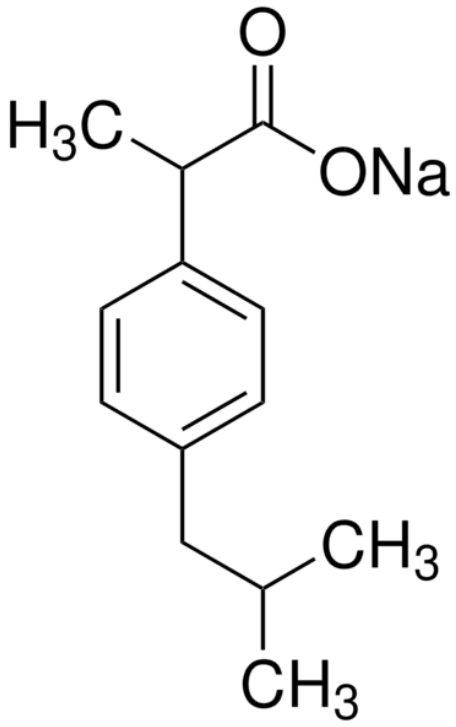

Figure 7. *Structure of ibuprofen sodium salt [29].*

Chemical formula: $C_{13}H_{17}O_2Na$.

Molar mass: 228.26 g/mol.

Ibuprofen belongs to the family of non-steroidal anti-inflammatory drugs. Its chemical formula has a benzene ring with a carboxylic acid group

(-COOH). As sodium salt, ibuprofen has an improved solubility in water.

2. Naproxen sodium salt (**Figure 8**)

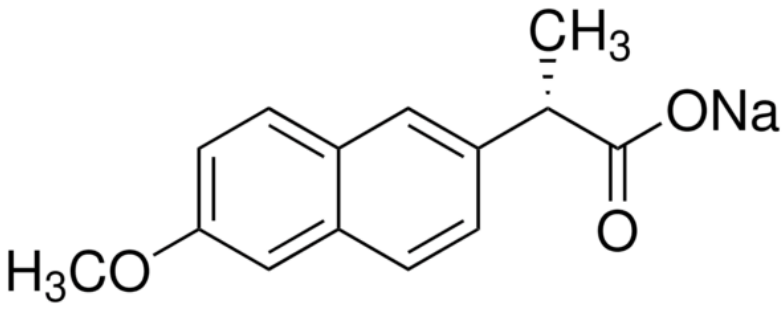

Figure 8. *Structure of naproxen sodium [30].*

Chemical formula: $C_{14}H_{13}O_3Na$.

Molar mass: 252.24 g/mol.

Also Naproxen belongs to the family of non-steroidal anti-inflammatory drugs. Its chemical formula has two benzene rings with a carboxylic acid group (-COOH). As sodium salt, naproxen has an improved solubility in water.

3. Gentamicin sulfate (**Figure 9**)

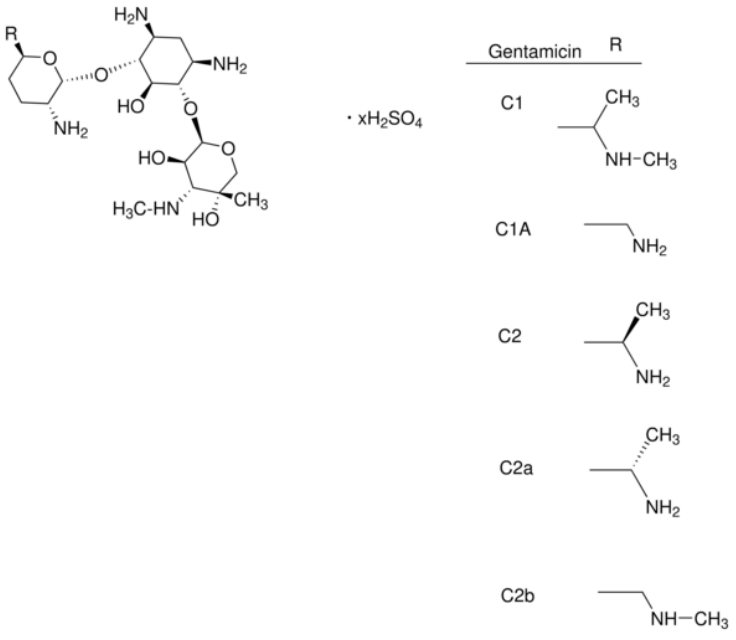

Figure 9. *General structure of gentamicin [31].*

The one used in the laboratory is gentamicin sulfate C1.

Chemical formula: $C_{21}H_{45}N_5O_{11}S$.

Molar mass: 575.7 g/mol.

Gentamicin is an aminoglycoside, broad-spectrum antibiotic. Gentamicin is composed of a series of amino sugars, and its structure has 3 glycosidic rings with amine groups [32]. Gentamicin sulfate is more soluble than pure gentamicin.

2.3 Characterization

Bone cements were characterized with:

- Fourier transform infrared spectroscopy (FT-IR), using both powder (ATR mode) and tablets (transmittance mode).
- TGA (thermogravimetric analysis);
- DSC (differential scanning calorimetry);
- Spectrophotometry.

Before and between each measurement made by these techniques, every machine and instrument used was meticulously cleaned using distilled water, ethanol and acetone.

Table 2 summarizes all the analyses done:

Table 2. *Summary of analysis made on the samples.*

Sample	IR (ATR)	TGA	DSC	IR on TGA sample	IR (transmittance)	Release test
1. Stoichiometric brushite	No	No	No	No	No	No
2. Brushite 1:1	No	No	No	No	No	No
3. Brushite 2:1	Yes	Yes	Yes	Yes	Yes	Yes
4. Brushite 3:1	Yes	No	No	No	No	No
5. Stoichiometric brushite + retardant (0,5 M)	No	No	No	No	No	No
6. Brushite 2:1 + retardant (0,5 M)	No	No	No	No	No	No
7. Brushite 3:1 + retardant (0,5 M)	Yes	No	No	No	No	No
8. Brushite 3:1 + retardant (1 M)	Yes	No	No	No	No	No
9. Stoichiometric brushite + retardant (1 M)	Yes	No	No	No	No	No
10. Brushite 2:1 + Ibuprofen 20%	Yes	Yes	Yes	Yes	Yes	Yes
11. Brushite 2:1 + Ibuprofen 10%	Yes	No	No	No	No	No
12. Brushite 2:1 + Naproxen 10%	Yes	Yes	Yes	Yes	No	No
13. Brushite 2:1 + Gentamicin 3%	Yes	Yes	Yes	Yes	No	No

The percentage is to be considered w/w.

2.3.1 Theory of the FT-IR

For the FT-IR spectroscopy was used the Thermo Nicolet 380 Nexus FT-IR spectrometer (**Figure 10**), with Omnic software, 100 scans, spectra expressed in terms of absorbance.

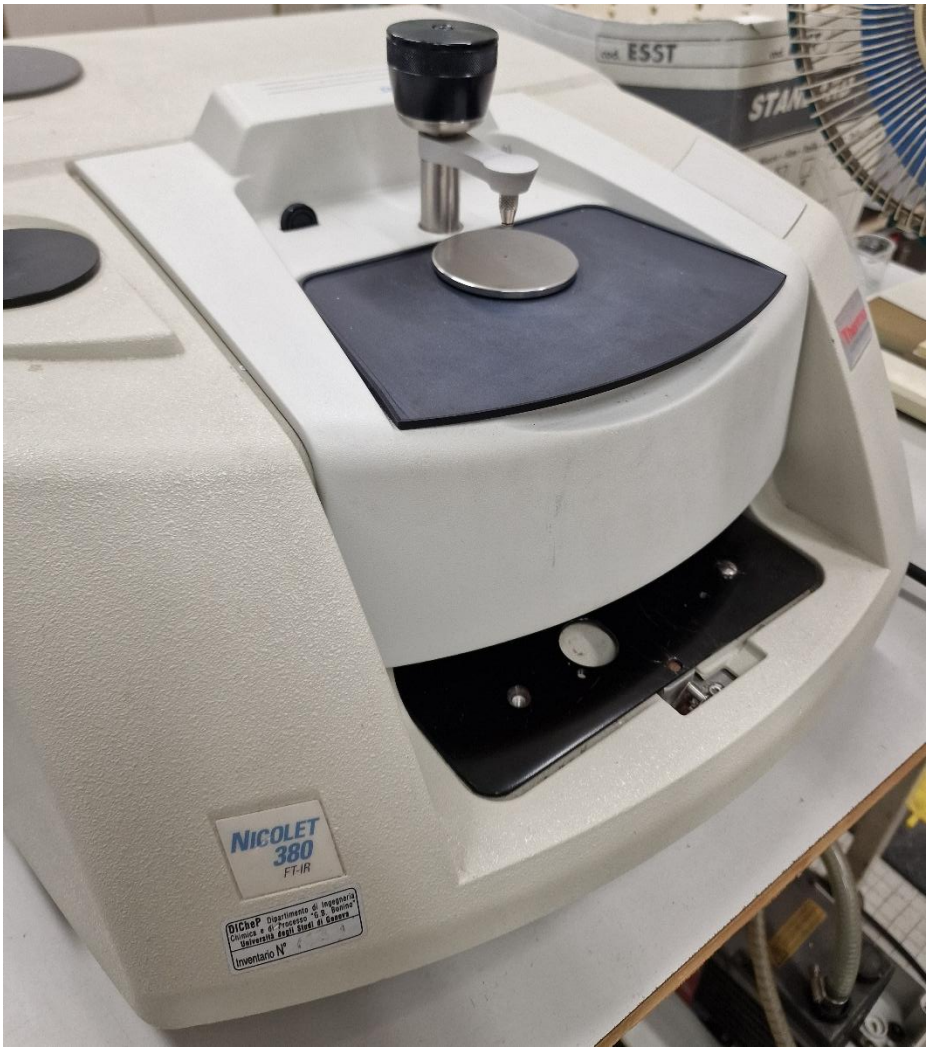

Figure 10. *Thermo Nicolet 380 Nexus FT-IR spectrometer.*

This analysis is based on the interaction of an electromagnetic radiation with matter, characterized by wavelength in the mid-infrared spectrum (500-4000 cm^{-1}). In this instrument there is the interferometer that allows specific wavelengths in a wide range of infrared radiation to be selected by interference. A fundamental principle on which IR spectroscopy is based is Lambert-Beer's law (1):

$$A = \varepsilon \, l \, C \quad (1)$$

Where:

- A [-] is the absorbance,
- ε [$M^{-1}cm^{-1}$] is the molar absorption coefficient;
- l [cm] is the optical path;
- C [M] is the concentration.

A can also be defined (2) as:

$$A = \log\left(\frac{I_0}{I_1}\right) = \log\frac{1}{T} \quad (2)$$

Where:

- I_0 is intensity of light emitted;
- I_1 is residual light intensity;
- T is transmittance.

Therefore, Lambert-Beer's law allows the quantification of absorbance. In fact, in the spectra that the measurement provides output, absorbance is measured as a function of wavelength.

With this technique, it is possible to learn more about the structure and functional groups of the sample. This analysis can detect variations in vibrational motions that correspond to an energy state. The main vibrations are:

- Stretching "*v*" of the bond or deformation, that can be symmetrical or not (this depends on whether the two atoms are simultaneously approaching or receding).

- Bending "δ" of the bond angle, that can be symmetrical or not (in or out of the plane of the bond angle).

A small amount of what was prepared was taken as a sample for the IR. Two measurements were made for each one. The interaction between the beam and the sample generate signals that are acquired by detectors. The latter are processed to form an image (**Figure 11**).

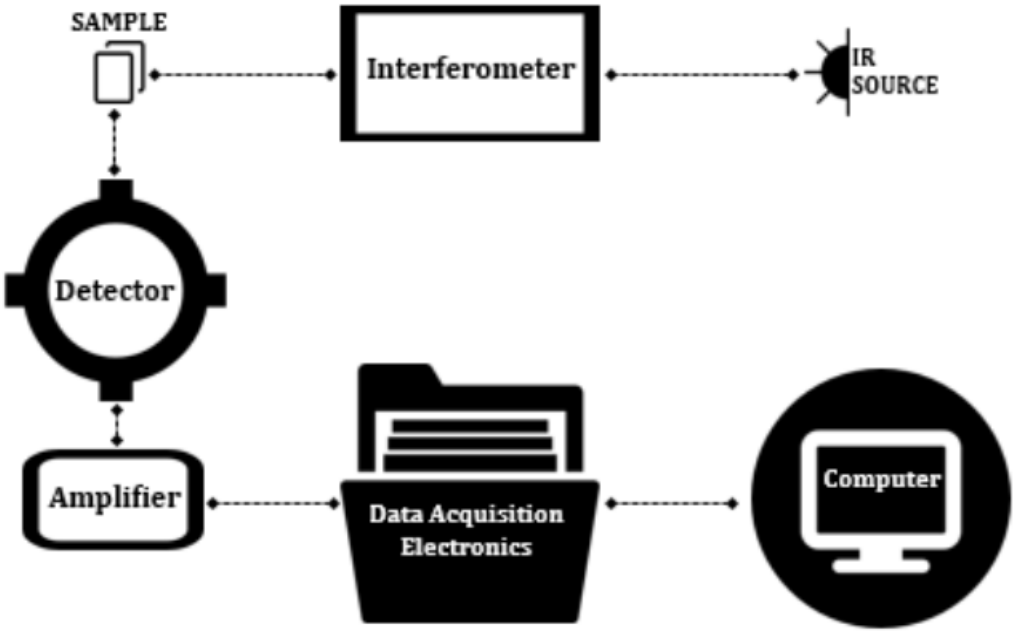

Figure 11. *FT-IR scheme [33].*

2.3.2 Practical application of FT-IR

The analysis methods are different and two were used in this case:

1. ATR mode, in this case the measurement path length is independent of sample thickness.
2. Transmittance mode [34].

In the first case, part of the bone cement sample was taken and analyzed as powder; in the second case, a tablet was made and studied. Tablets were prepared with the following samples: brushite 2:1 and brushite 2:1 + ibuprofen 20%. To these was added KBr (potassium bromide) to disperse them (**Figure 12**). The samples were mechanically mixed with the KBr with an agate mortar, that is chemically inert. For making the tablets 0.50 g of KBr and 0.01 g of the various samples analyzed were weighed. Thanks to a manual tablet press, round tablets were obtained. KBr was used because it does not affect the measurement because it appears to be transparent in infrared graph.

Figure 12. *Examples of tablets.*

First it should be done a background in air as a reference. Then the samples can be analyzed as powder or as tablets by placing them on special holders. Using this procedure, graphs were obtained for each sample.

Later, the brushite 2:1 and brushite 2:1 + ibuprofen 20% tablets were also analyzed with another home-made instrument created by the University of Genova laboratory (**Figure 13**). This instrument allowed the two samples to be studied through thermal ramps by IR in transmittance mode. It consists of an network of glass tubes in which air can circulates, it has several valves that can be closed or opened to create the vacuum. For the measurement made, the pressure was adjusted to about 765 Torr in air. The pipeline is connected to an oven into which the tablet is to be inserted on an appropriate holder. The sample remains a few minutes in the oven before being brought down to the lowest position seen in the figure and then analyzed with the FT-IR instrument.

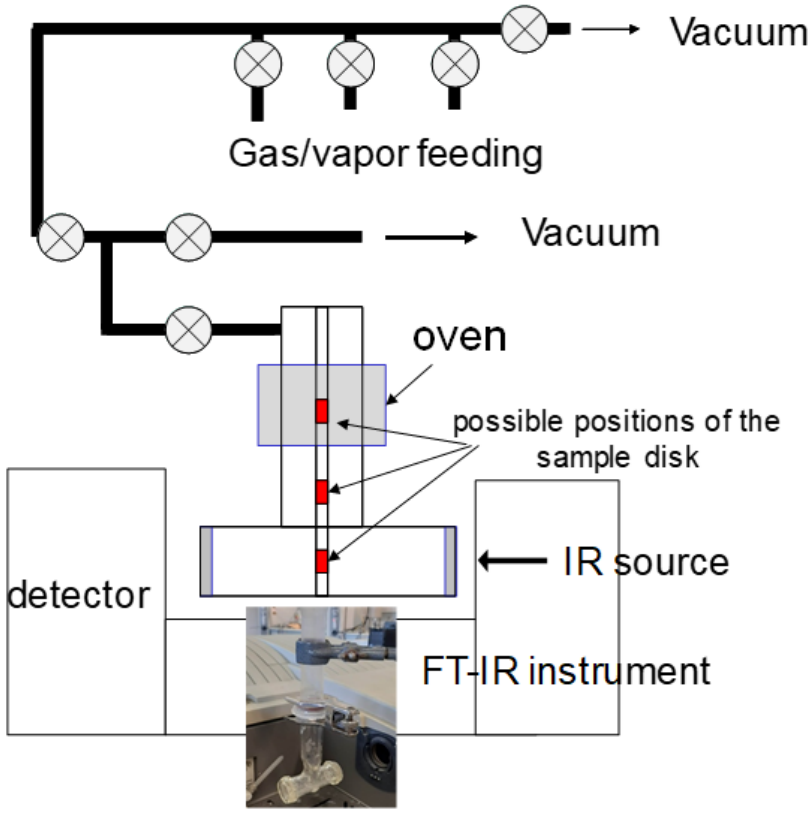

Figure 13. *Scheme of home-made instrument.*

The two tablets were subjected to heating in a temperature range of 100 °C to 400 °C and were analyzed every 50 °C to obtain the IR spectrum and thus see the evolution of the sample with the various temperatures. Again, background was always collected before the various measurements and the first one was done at the room temperature.

This analysis with the oven was executed to discuss the data obtained with the TGA.

2.3.3 TGA

Thermogravimetric analysis (TGA) measures the change in mass of a substance with a temperature cycle during a given time in a monitored atmosphere. This measurement allows identification of the pure organic versus inorganic decomposition peak, so the two decomposition temperatures can be observed to understand how they interact.

For the TGA several samples were prepared by taking material and weighing it in an analytical balance having accuracy to the tenth of a milligram. The different samples taken weighed about 70 mg to 120 mg.

The instrument used is STA Netzsch 409 thermobalance, it has single or dual holders and different types of sample holders and crucibles (sensitivity of 0.01 mg). It works with air. The crucibles used are made of alumina (**Figure 14**). The thermocouple used is type S, it consists of a platinum and a platinum-rhodium alloy (10%) filament joined at one end (hot junction), while the other end is connected to the measuring system. The temperature range used is from room temperature (25 °C) to 800 °C with a heating ramp-up programmed at 10 °C/min. The different tests last about an hour each. The data acquisition system was Netzsch 414/1 DAQ (Data Acquisition System) connected to a computer, it is connected with software to process the data.

DTA (differential thermal analysis) was also obtained with the same data. It is a measure the temperature difference that occurs between the analyzed sample and the reference sample over time. DTA is expressed in volt (V) because the operation of thermocouples allows a temperature difference to be translated into a potential difference. The DTA provides information about the physical and chemical processes occurring in the sample, establishing the temperature at which a given thermal phenomenon occurs and whether it is endothermic or exothermic.

Figure 14. *STA Netzsch 409 thermobalance.*

2.3.4 DSC

The DSC is a thermoanalytical technique, in this case the difference in the amount of heat required to increase the temperature of a sample and reference is measured as a function of temperature. It makes it possible to do a quantitative analysis. It was used Netzsch DSC 300 Caliris (**Figure 15**). Also in this case, samples were prepared by taking material and weighing it in an analytical balance (they are smaller than those of the TGA). The different samples weighed about 10 mg and in this case the crucibles are sealed. In this case, the crucibles used are made of aluminum.

Before taking measurement, the nitrogen tank must be opened. The tests last about one hour and twenty minutes each. The temperature range used is from room temperature (25 °C) to 500°C, at a rate of 20 K/min.

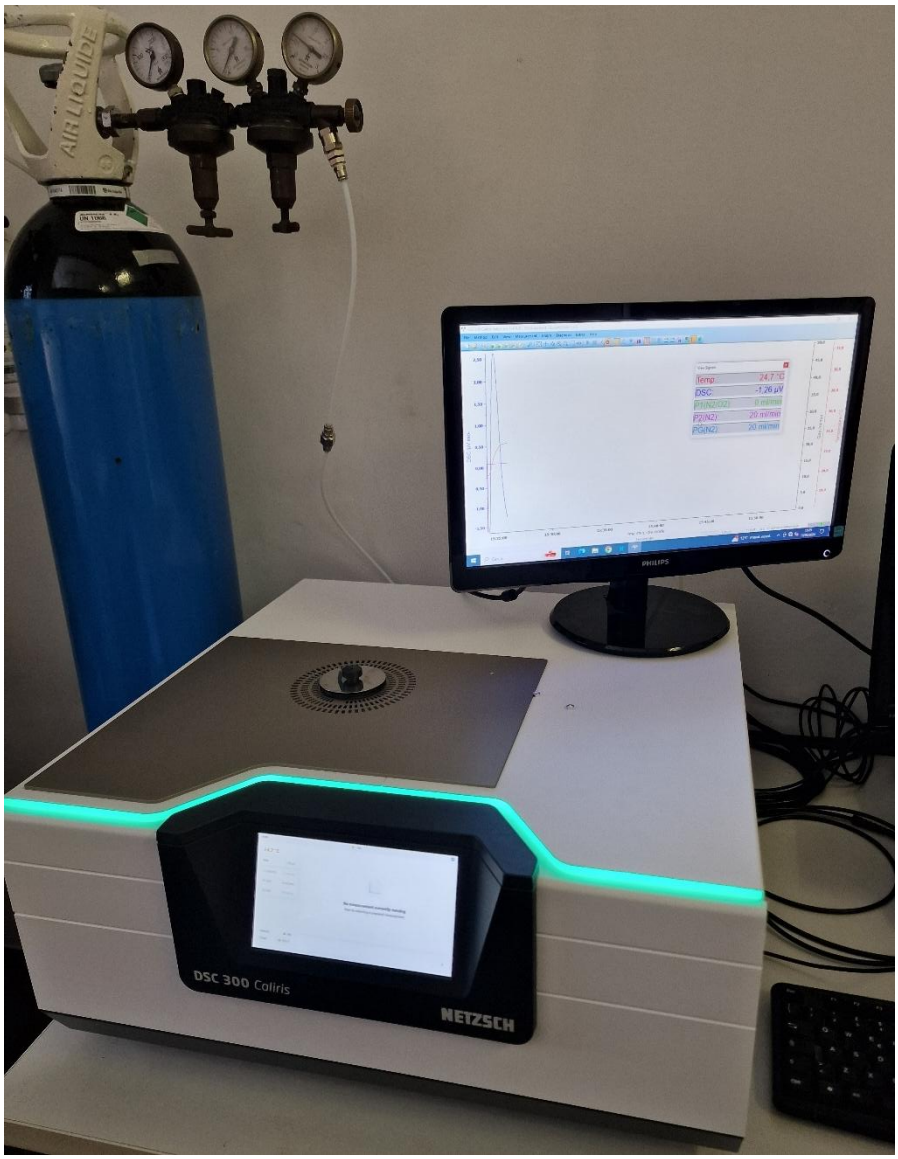

Figure 15. *Netzsch DSC 300 Caliris.*

2.3.5 Drug release

The study of drug release from bone cements is a key step in understanding the pattern that the chosen drug would have once implanted, with the cement, in the patient's body. Considering also the previous and literature studies, it was chosen to analyze the release of ibuprofen in the laboratory. The brushite 2:1 and brushite 2:1 + ibuprofen 20% samples were used to

carry out this study. The former was used as a comparison to understand the behavior of brushite over time. The samples were analyzed as time passed over a week to understand the evolution of the drug combined with bone cement.

The calibration curve method was used to obtain the release data. To obtain it, two pure ibuprofen samples were taken: A = 5.1 mg and B = 6.3 mg. Several dilute solutions with known concentrations of the considering molecule were prepared. This dilution was done in duplicate to have more data. The two samples were dissolved in PBS at a concentration of 2.5 mg/ml. PBS or phosphate buffered saline consists of a mixture of water and salts, its pH ranges from 7-7.4. This buffer solution helps maintain a constant pH, it is nontoxic and it is normally used for dilutions. PBS was used also as blank.

Starting from the stock solution of 2.5 mg/ml the following dilutions were made: 0.0125, 0.025, 0.05, 0.1, 0.2, 0.4, 0.5 mg/ml and 2 µL from each were taken. These were put on Nanoquant plate 16 flat black (**Figure 16**), which is part of the Tecan Spark, and were analysed with the spectrophotometer. Then a brushite 2:1 sample to which 250 µL of PBS was added was also analyzed in the same way. All samples were placed in eppendorfs. For each, absorbance was measured two times and then the mean of the values was considered. This curve allowed the different concentrations to be estimated by knowing the absorbance value at a given wavelength, which in this case was 222 nm. Whith this method, the different absorbance values were obtained.

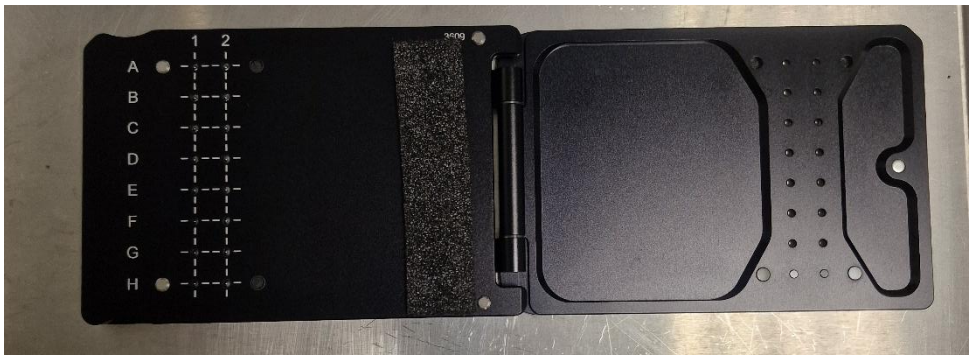

Figure 16. *Nanoquant plate.*

Subsequently, the samples were frozen at -20°C and then thawed and re-analysed using the same protocol before studying the release of ibuprofen from the brushite.

Tecan Spark® (**Figure 17**) was used to carry out spectrophotometry analysis.

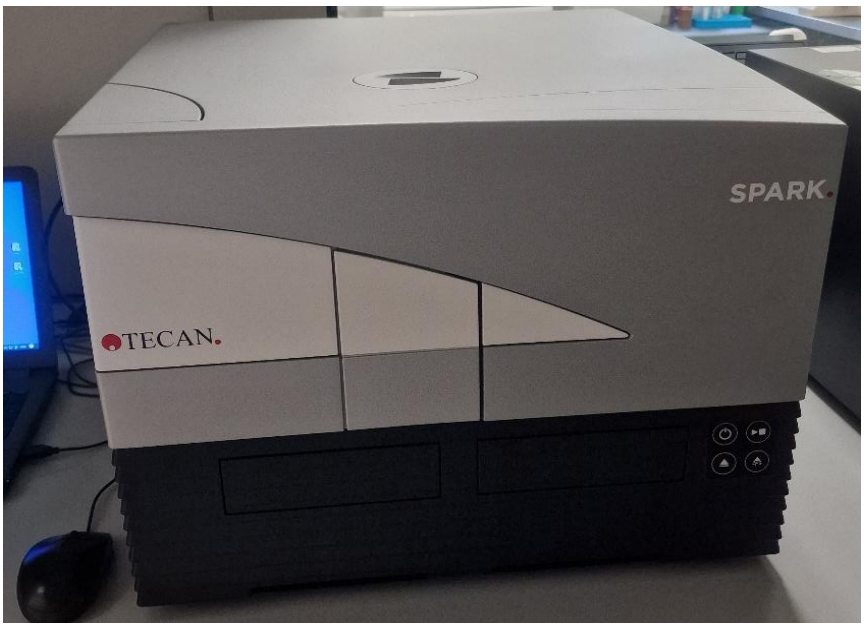

Figure 17. *Tecan Spark [35].*

This type of analysis is part of optical methods. UV-Vis spectrophotometry measures the amount of discrete wavelengths of UV or visible light absorbed or transmitted through a sample relative to a reference that is called a "blank". In this case, the beam of light comes from a UV/VIS source. It is sent through a monochromator that separates a particular wavelength radiation that is then directed into the sample. At the end, the intensity of the remaining radiation is detected by a light sensor. This is how the transmittance of the considered wavelength is measured. In fact, the Lambert-Beer's law also applies here. This technique provides information about the content of the sample and its concentration. Thanks to spectroscopy, it was possible to determine the quantitative levels of ibuprofen released [36].

To analyze the release, three samples of 2:1 brushite, each of approximately the same weight, and three samples of 2:1 brushite + 20% ibuprofen, also with the same weight, were weighed. The single brushite is used as a comparison to understand the true release of ibuprofen over time. PBS was added to the 6 samples and they were placed in eppendorfs. Solid/liquid ratio=1/10 was chosen. Again, pure PBS was used as a blank (1.5 ml).

The samples are shown in **Table 3**:

Table 3. *References.*

Sample	Solid [g]	Liquid [ml]
1. Brushite + ibuprofen	0.1462	1.462
2. Brushite + ibuprofen	0.1395	1.395
3. Brushite + ibuprofen	0.1406	1.406
1. Brushite	0.1424	1.424
2. Brushite	0.1442	1.442
3. Brushite	0.144	1.44

To study drug release, the samples were stabilized in an agitator (Robbins Scientific Rotary® Blood Mixer / Agitator) that made 12 rpm (**Figure 18**).

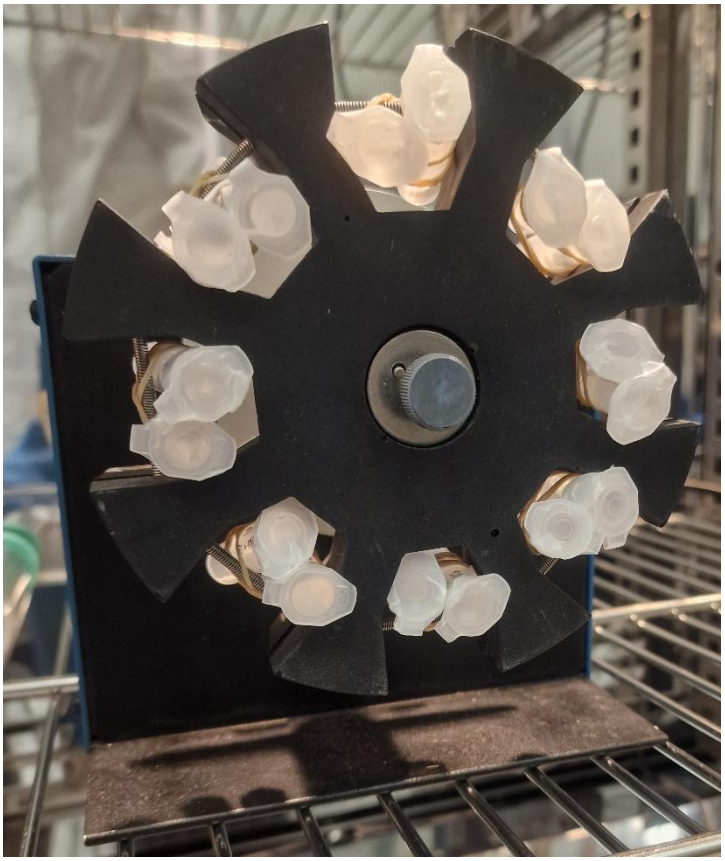

Figure 18*. Robbins Scientific Rotary Blood Mixer / Agitator.*

It was placed in a VWR incubator (Randor, PA, USA) at a temperature of about 37°C to simulate human body conditions. Over a one-week period, several samples were taken from these six mentioned above and each time an amount of liquid equal to 10% of the solution was taken and the same amount of PBS was added back. Sampling was done after: 5, 10, 15, 30 minutes, 1, 2, 3, 22, 24, 26, 28, 96, 100, 120, 144, 168 hours.

Afterwards, the samples either were analyzed immediately with the spectrophotometer or were frozen at -20°C and analyzed later. Each time before spectrophotometer analysis, each sample was centrifuged (Centrifuge 5415 R, 16000 xg, for 10 minutes, 4°C). Again, to obtain absorbance values, 2 μL was taken to be placed on the Nanoquant plate. To get the concentration of ibuprofen, on the same day that spectrophotometer analysis was done, the calibration curve was also analyzed by thawing the samples.

3. Results and discussion

Using the methodologies described in the previous chapter, a series of samples were obtained and the release system was also studied. The main results are given in the chapters below.

3.1 Sample workability

It was observed that in samples prepared with sodium citrate the cement phase was more workable and allows the reaction temperature to decrease. During the preparation of the various samples, it was observed that even ibuprofen had a delayed action, while both naproxen and gentamicin had a less obvious slowing of the setting time.

Going into more detail, slightly different setting times were observed during different preparations. For single brushite, the stoichiometric preparation does not even leave time for mixing. The 3:1 preparation turns out to be more workable because the setting time is slightly higher, but it is still a difference of minutes. Same thing applies to the preparation with sodium citrate and it turns out to be better the one with 0.5 molar retardant.

For preparations with ibuprofen, the most workable is 2:1 with 10% of it. For naproxen only the 2:1 one with 10% drug was made and for gentamicin only the one with 3% antibiotic. Regarding the last two cases, no significant delays in bone cement setting time were found with these concentrations.

3.2 FT-IR Spectra

The IR analysis was done on the samples mentioned in **Table 2**, each measurement was repeated but only individual cases will be reported as examples for discussion. The spectra obtained allowed identification of brushite, retardant and drug phases used. The main vibrations of the compounds that will be mentioned and their explanations have been given in chapter **2.3.1 Theory of the FT-IR**.

1. IR spectra of brushite and brushite + retardant

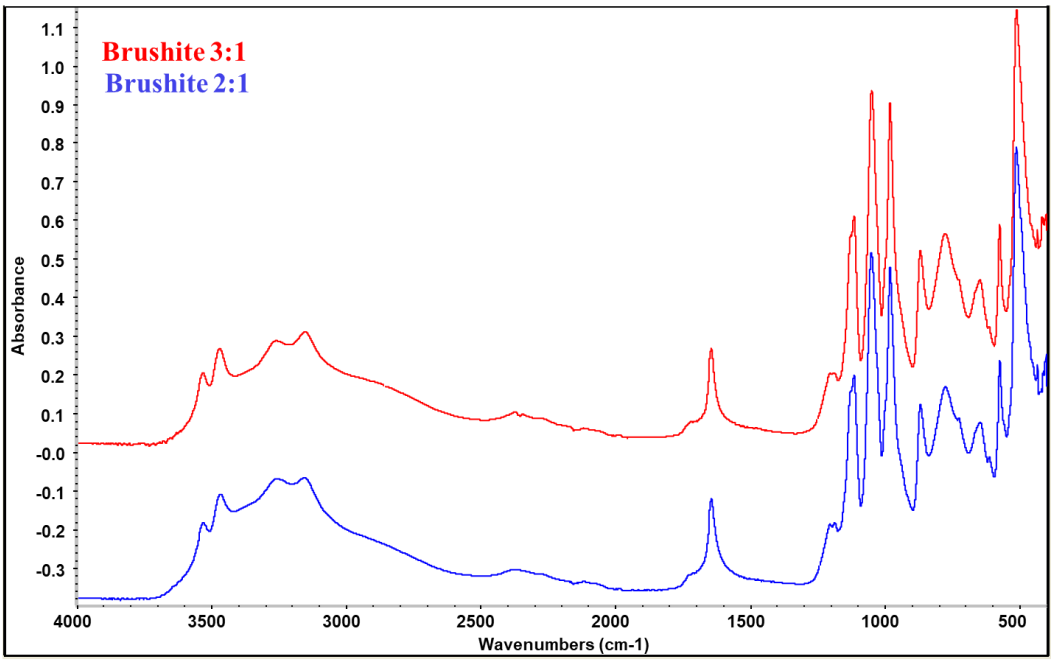

Figure 19. *FT-IR Spectra od brushite 2:1 and 3:1 (common scale).*

The two spectra of the 2:1 and 3:1 brushite can be seen in **Figure 19** and the typical bands of the material considered are found. Despite the fact that brushite is a crystalline material, it is possible to assign the different vibrational modes it has to groups specific: hydrogen phosphate (HPO_4) groups and crystallization water. The former have three groups of vibrations: stretching $\nu(PO_4^{3-})$, OPO bending and one group of vibrations, due to the vibrational mode of the OH. Instead the water

molecule δ(H_2O) has two vibrations: internal vibrations and libration modes [37].

The difference between the spectra of the two samples (2:1 and 3:1) is minimal. In the figure the bands of phosphate groups (PO_4^{3-}), in the range between 800 cm^{-1} and 1200 cm^{-1}, known from the literature are assigned to the stretching of the bonds of the phosphate group [38]. PO stretching modes are intense and well separated and there are no other bands of different groups in this frequency. The vibrational mode of PO bonds can be observed also in the region between 400-600 cm^{-1}. Since brushite is a hydrated compound, both hydrogen bonds and van der Waals interactions are important. The crystallization water is characterized by these bands: the high-frequency doublet around 3500 cm^{-1}, the band below 3300 cm^{-1} and a deformation band around 1650 cm^{-1} [39].

The bands shown above are comparable with those shown in the table below (**Table 4**), which is part of an experimental study.

Table 4. *Experimental data of IR brushite [37].*

a) Intensity: s=strong, m=medium, w=weak, v.w=very weak, and sh.=shoulder.

b) Experimental assignment in ref 18 at 77 K.

c) Experimental assignment in ref 17 at 77 K.

		experimental	
vibrating species	assignment	frequency[b]	intensity[a]
HPO_4	H-stretch	2950	m.sh
	H-in-plane bend	1210	m
	H-out-of-plane bend	792,750	s,sh.
	PO stretch	1137	s
		1125	sh
		1068	sh
		1058	s
		1000	sh
		987	s
		880	m
		870	sh
	OPO Bend	579[c]	s
		542	sh
		527	s
		445	m
		420	sh
H_2O	stretch W(2)	3522,3530	s,w.sh
		3471,3460	s,sh
	stretch W(1)	3275,3240	s,sh
		3150,3135	s,sh
	bend W(1)	1650	m
	bend W(2)		
	libration W(1)		
		675	m
	libration W(2)	665	sh
		612	v.w

Knowing this, it will be clear that in all the underlying spectra with brushite, its typical bands can be identified. This confirms that brushite was always obtained in every preparation made.

2. IR spectra of brushite and brushite + retardant (sodium citrate)

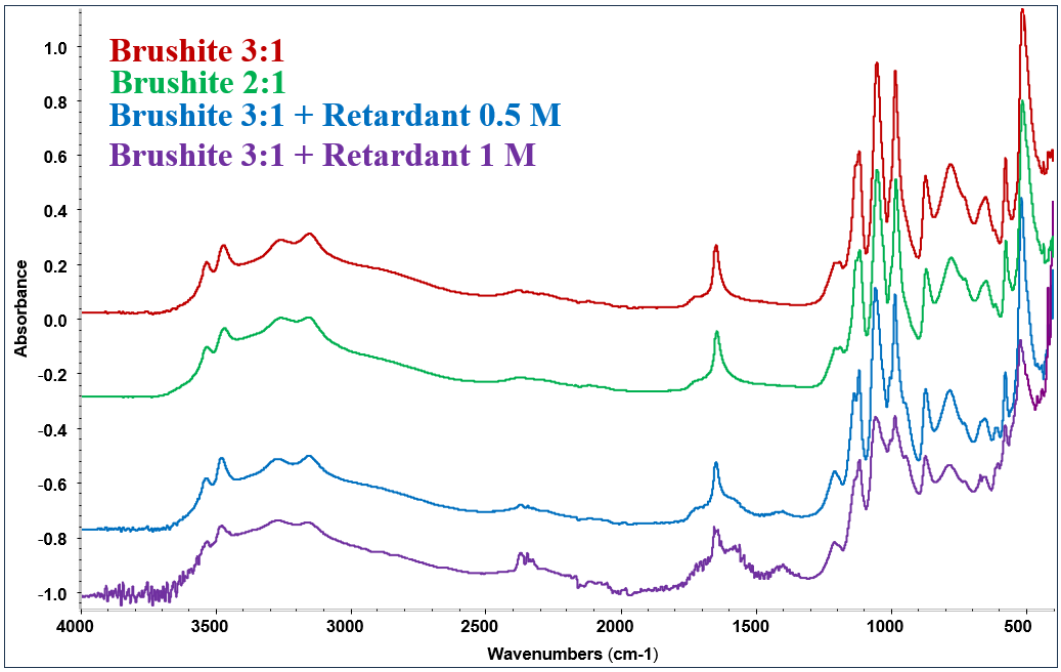

Figure 20. *FT-IR Spectra of brushite 2:1 and 3:1, brushite 3:1 + retardant 0.5 M and 1 M (no common scale).*

In regard to the retardant, sodium citrate, it can be seen (**Figure 20**) that it does not completely change the brushite spectrum but attenuates the PO_4^{3-} bands, especially the 1 M. The broad and weak signals present between 1410 and 1590 $cm^{-1}$are due to retardant residues. They are due to the stretching modes of the COO^-carboxylate group.

Hydration water is seen around 1650 cm^{-1}. The fact that some bands are more intense in the 1 M sample is because it has more sodium citrate. With 0.5 M and 1 M, the peak around 1650 cm^{-1} is less prominent and this could be due to less water of crystallization. In addition, another less visible peak appears near 1400 cm^{-1}, more evident with 1 M.

3. IR spectra of brushite, brushite + ibuprofen

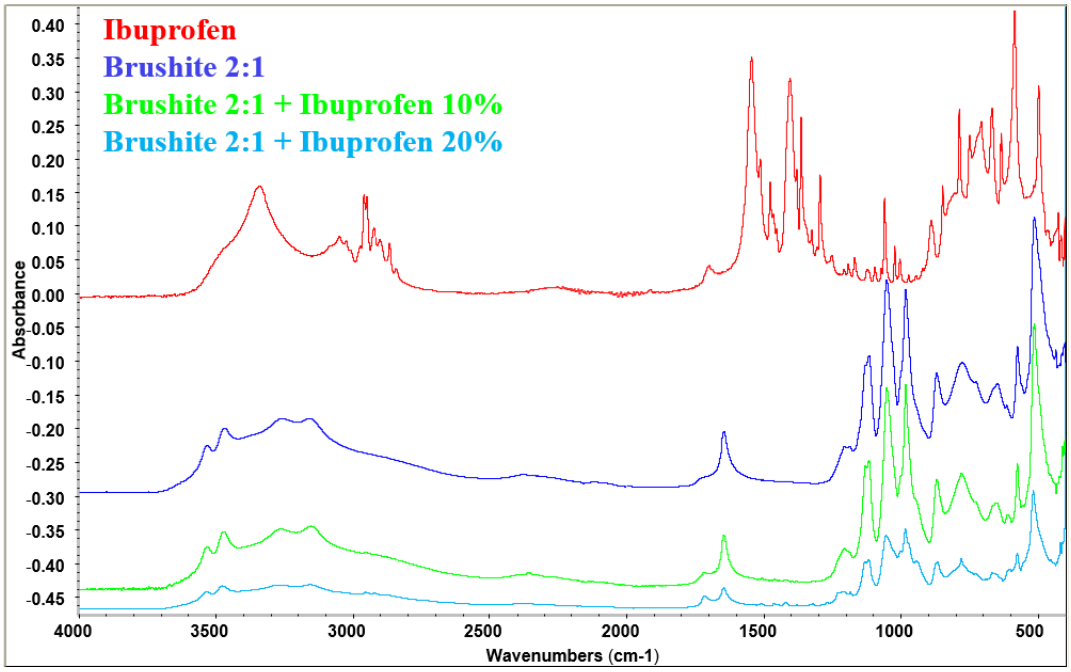

Figure 21. *FT-IR Spectra of ibuprofen, brushite 2:1, brushite 2:1 + ibuprofen 10% and 20% (no common scale).*

These spectra (**Figure 21**) show that the addition of ibuprofen to brushite did not alter its preparation since the typical bands of brushite are all present. The higher percentage of the drug makes those of ibuprofen more evident even when bound with the matrix. Characteristic bands of ibuprofen: stretching ν(C=O), stretching ν(C-H) and CH bending.

The spectra reported in figure show the bands changing and developing due to the interaction between brushite and ibuprofen. It can be seen how some typical peaks of the drug (500 cm^{-1} and 1000 cm^{-1}) were attenuated by bonds to bone cement. Other bands that can be assigned to the drug can be seen in the low frequency region, around 1700 cm^{-1} are those of the ibuprofen C=O stretching mode. This confirms that the carboxylic group is still present after interaction with the brushite. From the figure it can be seen with this band is more evident in the case of ibuprofen at 20%. Same for the bands between 800 cm^{-1} and 1400 cm^{-1}, they are due to CH deformation and CC deformation/stretching modes of the molecule. The band at 1508 cm^{-1} is due to the aromatic ring vibrational modes.

These bands are completely consistent with bands of pure ibuprofen. Thus, it is suggested that the interaction occurs on the pore surface and the outer surface through weak bonds. For example, the broadening of the band due to C=O in the hydrophilic part of the molecule could indicate the formation of H bonds with the OH of the inorganic structure. This can be seen by observing the decrease in the intensity of the crystallization water bands between 3000 and 3500 cm^{-1}, especially with ibuprofen at 20 %. Same goes for the peak around 1650 cm^{-1} [40].

In the composite spectra bands due to ibuprofen are very weak, thus in order to enhanced features of the organic molecules the subtraction spectra were analyzed.

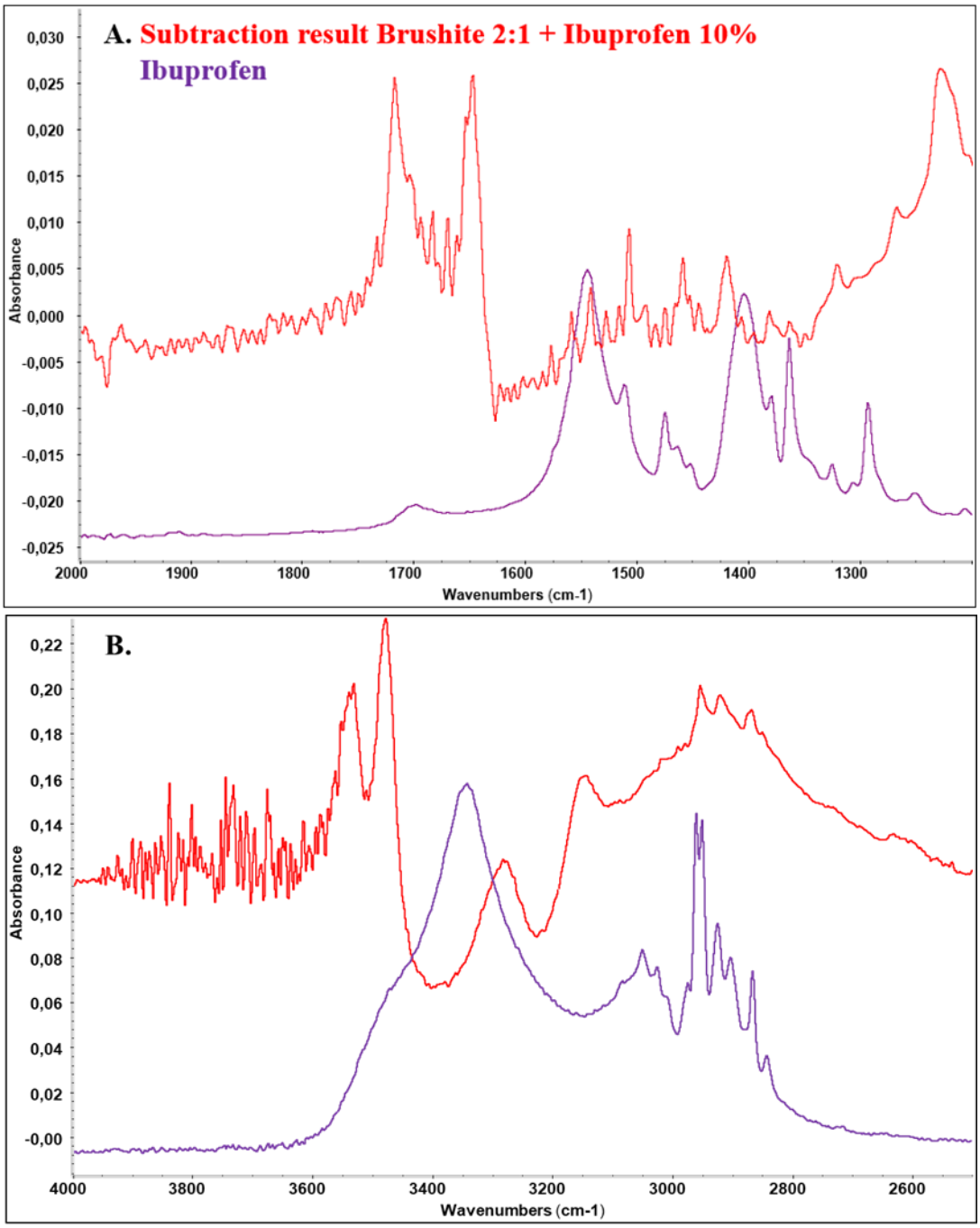

Figure 22. *FT-IR Subtraction spectra of brushite 2:1 + ibuprofen 20% and ibuprofen. The spectrum of brushite 2:1 has been subtracted from that of brushite 2:1 + ibuprofen 10%.*

A) Low frequencies. B) High frequencies.

For this analysis, subtraction was made between the brushite 2:1 + ibuprofen 10% spectrum and the brushite 2:1 spectrum and then compared with ibuprofen (**Figure 22**). This spectrum has been divided into two:

A. At 1200-2000 cm^{-1} there are weak bands so ibuprofen is found in the form of free acid and COOH group. The most evident

is at 1720 cm^{-1} and is the stretching C=O of the carboxylic group as discussed previously. At 1400 cm^{-1} there is the one band of pure ibuprofen while at 1420 cm^{-1} the bands of brushite + ibuprofen are overlapped. The two just mentioned and the one at about 1540 cm^{-1} represent the stretching of the COO^- group of the, thus the carboxylate. From 1450 to 1520 cm^{-1} there are the bands due to CH deformation of the aliphatic $CH_2 - CH_3$ chain and the aromatic ring. At 1452, 1465, and 1475 cm^{-1} are the δCH and CH-chain strain bands of ibuprofen. There may be a carboxylate residue whose main bands are shifted relative to the reference bands. The peak at 1545 cm^{-1} disappears and one goes from 1404 cm^{-1} to 1418 cm^{-1}. This can be explained by acid pH of the sample and considering that ibuprofen sodium salt was used. In fact, other studies have shown that the pH decrease during formation of brushite, which leads to the formation of free COOH groups in the acidic form of ibuprofen [41]. This affects the pH of bone cement and results in the displacement and appearance of new bands such as those around 1700 cm^{-1} for that of COOH.

B. The bands between about 2800 cm^{-1} and 3100 cm^{-1} are due to CH stretching.

Bands that are negative represent something that was in brushite and that has changed, for example that of water because molecules have decreased.

4. IR spectra of brushite, brushite + naproxen

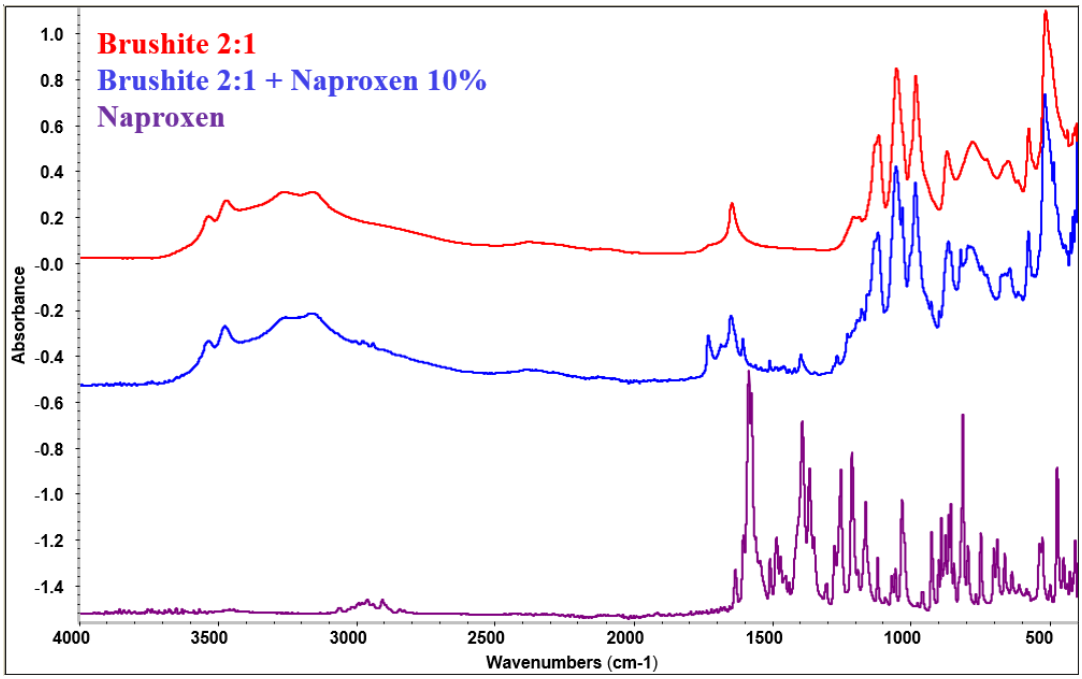

Figure 23. *FT-IR Spectra of brushite 2:1, brushite 2:1 + naproxen 10% and naproxen (no common scale).*

This spectra in **Figure 23** show that the addition of naproxen to brushite did not alter its preparation since the typical bands are all present. The characteristic bands of naproxen are: stretching ν(C=O) and stretching ν(C-H).

Naproxen has a strong band between 1500 cm^{-1} and 1600 cm^{-1} due to the stretching C=O of the carboxylic group. This drug shows also bands between 2800 cm^{-1} and 3000 cm^{-1} due to CH bonds. At 1504 cm^{-1} and 1602 cm^{-1} there is the C-C bond stretching band. Phosphate bands of brushite and drug bands interact and this results in alterations, while those related to the C=O and CH groups of naproxen could show small shifts or changes in intensity.

Next, the subtraction spectra were analyzed.

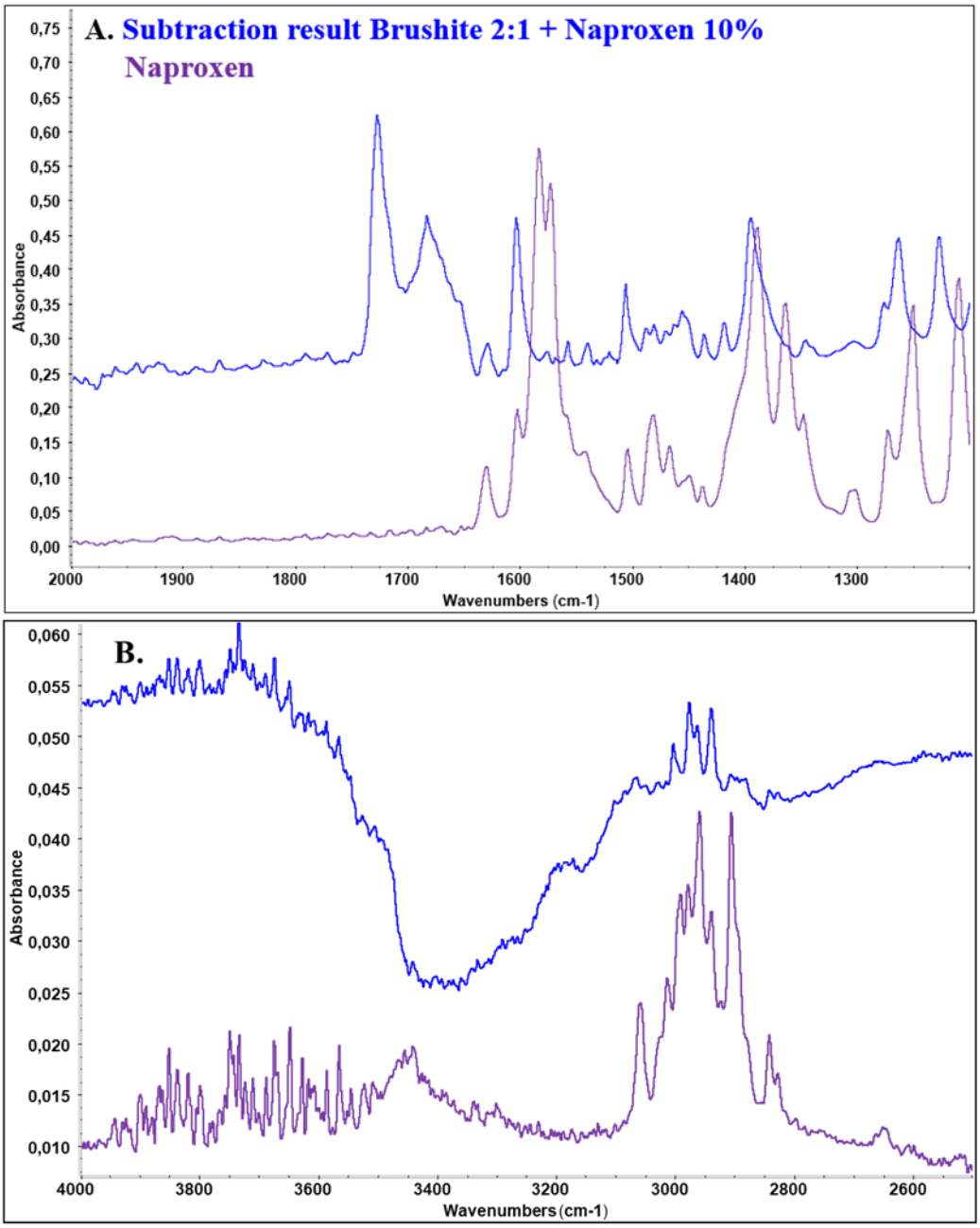

Figure 24. *FT-IR Subtraction spectra of brushite 2:1 + naproxen 10% and brushite 2:1. The spectrum of brushite 2:1 has been subtracted from that of brushite 2:1 + naproxen 10%. A) Low frequencies. B) High frequencies.*

In this case, subtraction was made between the spectrum of brushite 2:1 + naproxen 10% and brushite 2:1, the result was compared with naproxen (**Figure 24**). During brushite formation, the compound that was a sodium salt (the naproxen used) is found in acid form, and this results in some changes among the spectra. This spectrum has been divided into two:

A. At 1200-2000 cm^{-1} there are weak bands. Again the typical band of free COOH appears. The bands at 1580 cm^{-1} and 1730 cm^{-1}

are clearly modified by interaction with the matrix. The CH area has also changed compared to the case with ibuprofen because naproxen is a stiffer and bulkier molecule. At 1200-1300 cm^{-1} the bands are shifted. Here the 1504 and 1602 cm^{-1} peaks disappear and the one at 1727 cm^{-1} of a COOH due to acidity appears. Again, the same explanation about the influence of pH made for ibuprofen can be made here [41]. In fact, naproxen sodium salt was used.

B. At 2800-3100 cm^{-1} CH and aromatic ring stretches are clearly evident.

5. IR spectra of brushite and brushite + gentamicin

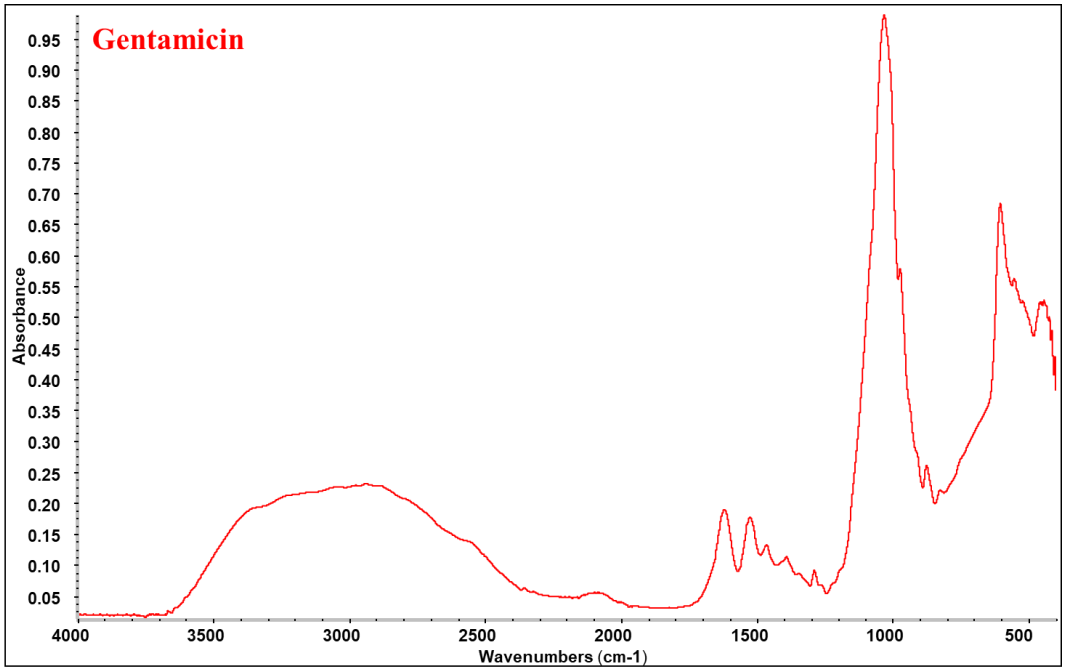

Figure 25. *FT-IR Spectrum of gentamicin.*

In spectrum of gentamicin sulfate (**Figure 25**) different peaks can be detected. It has some characteristics bands like the one related to cyclic amines or amine groups linked to an aliphatic ring: 1530 cm^{-1} and 1630 cm^{-1} [42].

The broad diffuse band between 2500 cm^{-1} and 3600 cm^{-1} is explained by the presence of numerous antibiotic molecules interaction. In particular the bands at 3400 cm^{-1} and 2960 cm^{-1} correspond to the NH and alkyl CH stretching vibrations. The strong absorption band between

900 cm^{-1} and 1300 cm^{-1} corresponds to the stretching vibrations of CN and also to numerous stretching vibrations of C-O group.
There is also HSO_4^{-1} vibrational band at 1114 cm^{-1}. The S-O bending and stretching vibrations are at 610 cm^{-1} and 1051 cm^{-1}respectively, they are attributed to the sulfur content of this drug [43].

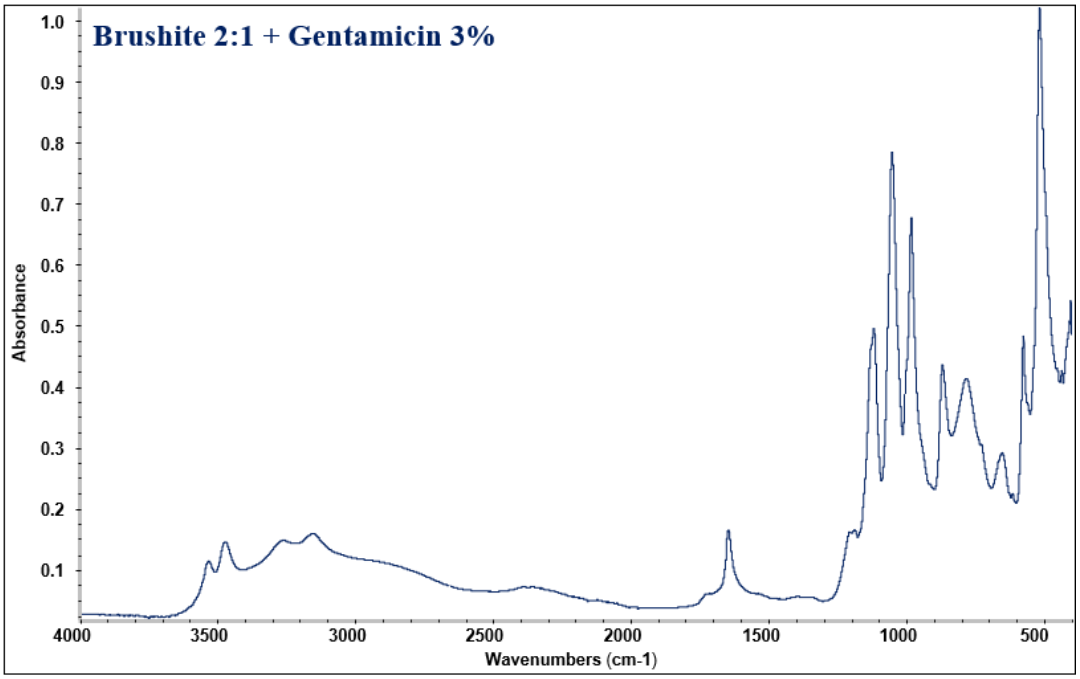

Figure 26. *FT-IR Spectrum of brushite 2:1 + gentamicin 3%.*

When gentamicin interacts with brushite, the same bands mentioned above for the single brushite sample can be seen (**Figure 26**). No major changes are observable, and this is due to the low percentage of gentamicin used.

3.3 Thermal evolution

Regarding the analysis on the thermal evolution of the samples, the results of TGA, DSC, and oven analysis on the samples mentioned in **Table 2** will be reported. It should be specified that TGA was carried out with air while the DSC in inert atmosphere with nitrogen, this results in the presence of differences in the plots obtained. For example, in the case of DSC analysis there is no oxidation.

1. TGA brushite

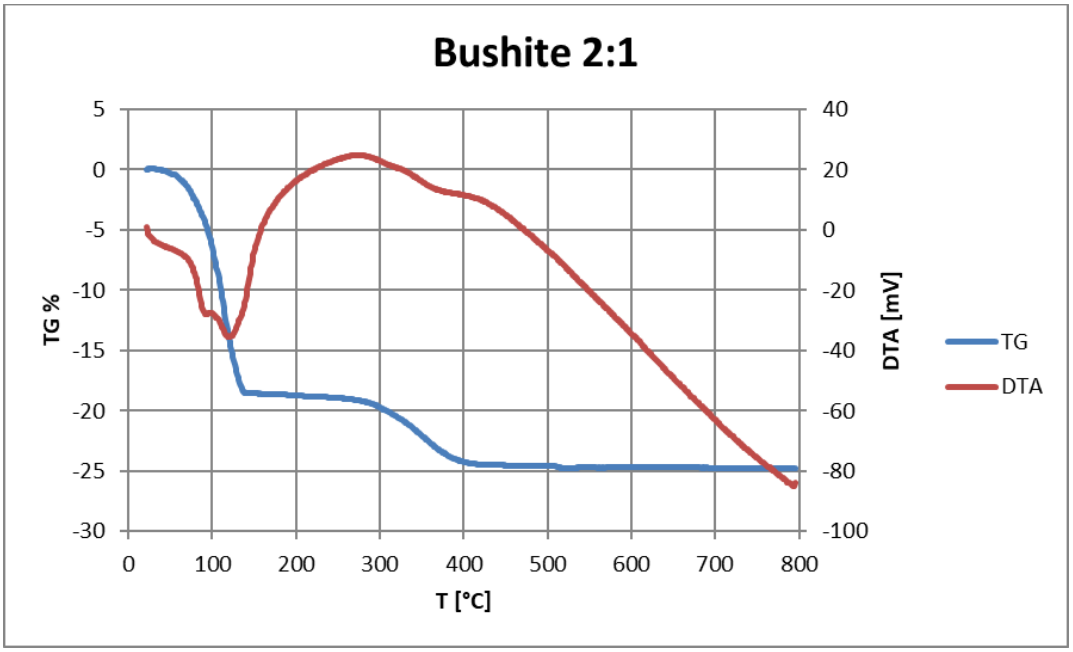

Figure 27. *TGA brushite 2:1.*

From the plot (**Figure 27**) of the brushite 2:1 sample (104.8 mg), three endothermic peaks located at about 94 °C, 122 °C and 367 °C can be seen (visible thanks to DTA, downward peaks are endothermic). The first two represents the transition from brushite to monetite, which is its anhydrous form, this is the result of the loss of water of crystallization The third represents the transition to calcium pyrophosphate. They correspond to a mass loss (visible thanks to TGA) of about 18% w/w for the first two, between 22 °C and 144 °C , and about 5% w/w in the latter, between 300 °C and 400 °C.

As mentioned earlier, this is one of the samples on which thermal analysis was followed also by IR spectroscopy with the apparatus described in chapter **2.3.2 Practical application of FT-IR**, in order to compare it with TG and further verify the evolution of the materials with temperature. From the IR in transmittance mode of the tablet, the following spectra were obtained:

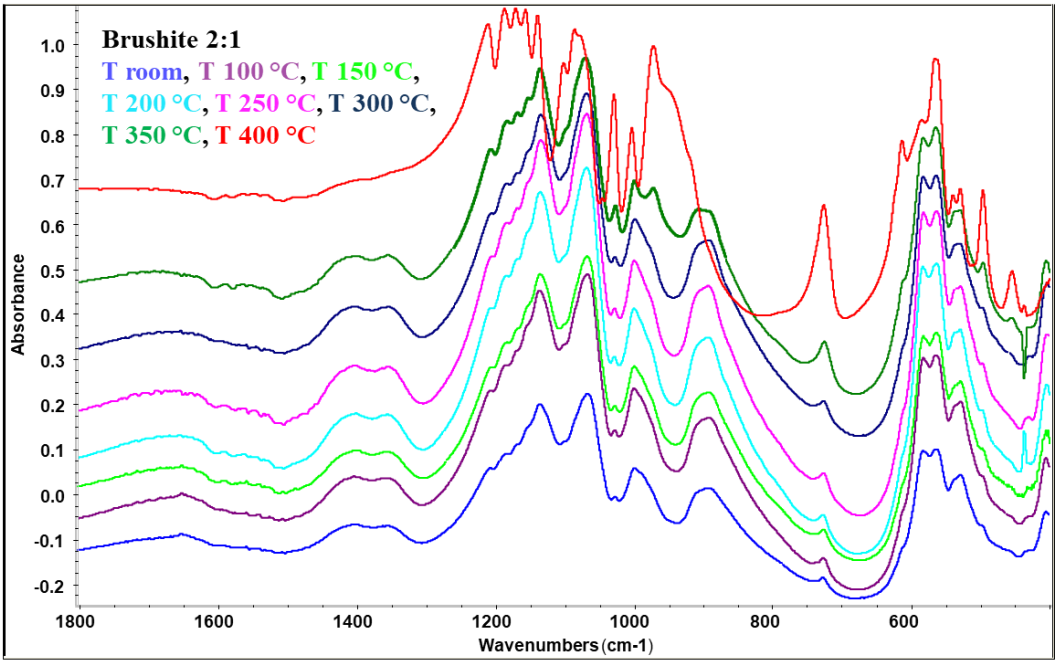

Figure 28. *FT-IR Spectra of brushite 2:1 at different temperatures increasing from the bottom (no common scale).*

The focus was on the frequencies between 400 and 1800 cm^{-1} (**Figure 28**). Thus, the thermal evolution of the phosphate groups (PO_4^{3-}) can be observed. During the increase in temperatures there was the transition to calcium pyrophosphate. The two temperatures where there is a real change in the spectrum are 350 °C and 400 °C [39]. The results obtained from this analysis are consistent with those of TGA.

2. TGA ibuprofen and brushite + ibuprofen

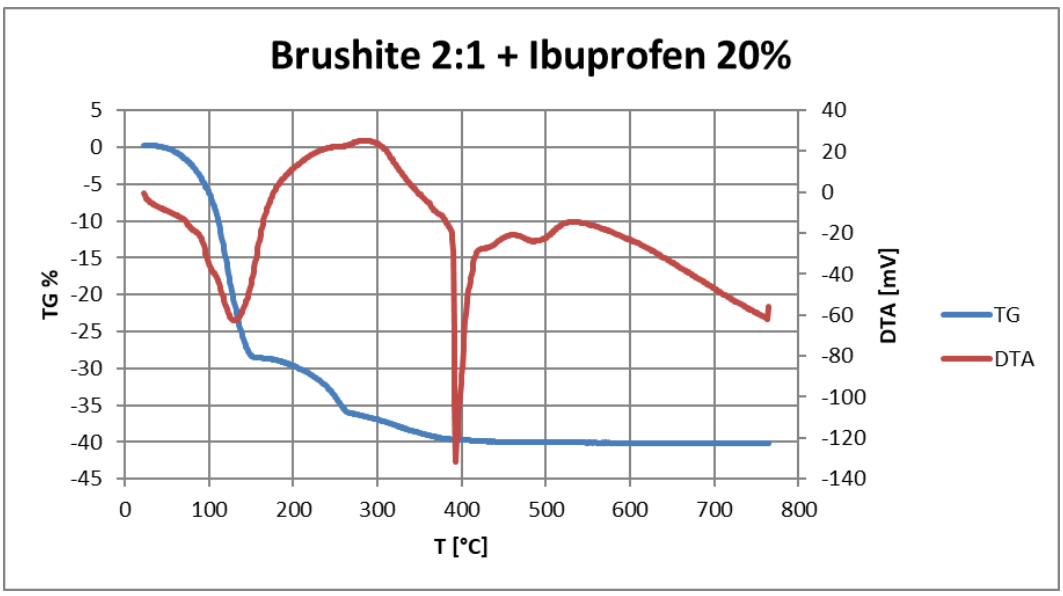

Figure 29. *TGA brushite 2:1 + ibuprofen 20%.*

For the brushite 2:1 + ibuprofen 20% sample (124.1 mg), there are three endothermic peaks (**Figure 29**): 132 °C, 393 °C and 495 °C, respectively. For the former the mass loss is about 28% w/w in a range between 23 °C and 160 °C, for the second is 3% w/w in a range between 276 °C and 400 °C while for the latter it is minimal.
Again, the first peak could correspond to the transition from brushite to monetite, combined with the beginning of ibuprofen degradation. The second is almost certainly due to the transformation to calcium pyrophosphate.

In the first case, brushite might act as a catalyst for the initial degradation of ibuprofen by lowering its temperature. In fact, evaporation of ibuprofen begins at about 152°C and is followed by endothermic degradation, so it is the brushite that acts by delaying this phenomenon [44].

This can be confirmed by looking at the degradation of ibuprofen.

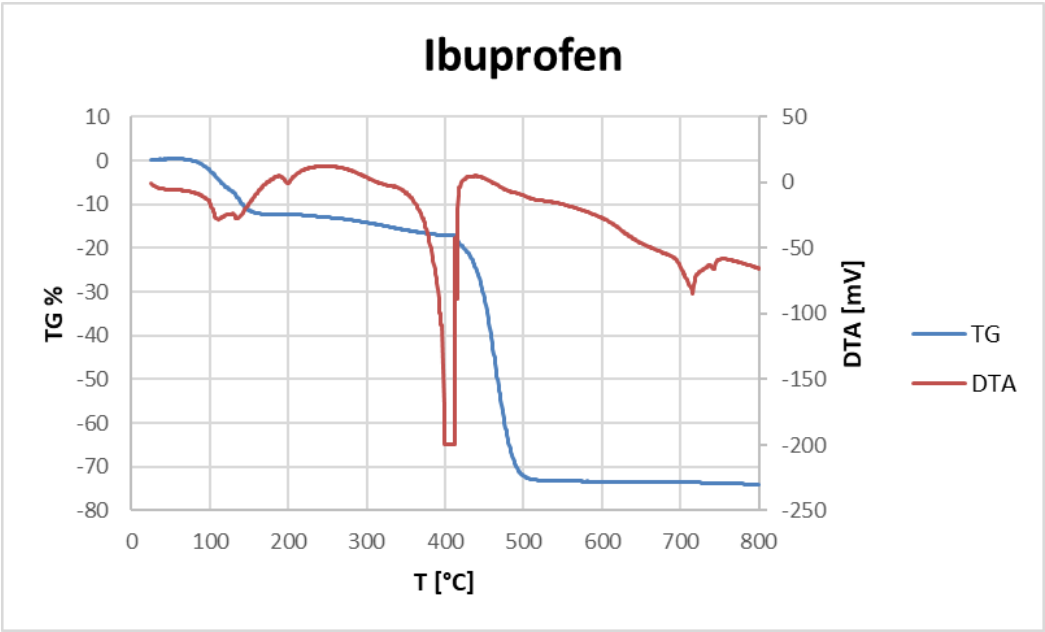

Figure 30. *TGA ibuprofen.*

The drug sample (81 mg) has several endothermic peaks (**Figure 30**): 113°C, 130°C, 199°C, 404°C, 715°C and 738°C. Overall for the first three there is a mass loss of about 12% w/w in a range between 25 °C and 200 °C (the point at 152°C mentioned earlier is included in this range). In the fourth case the mass loss is about 28% w/w in a range between 307 °C and 413 °C while for the last two it is minimal.

Brushite 2:1 + ibuprofen 20% is the second sample on which the thermal analysis was done with IR spectroscopy. The spectra obtained with IR in transmittance mode are reported in **Figure 31**:

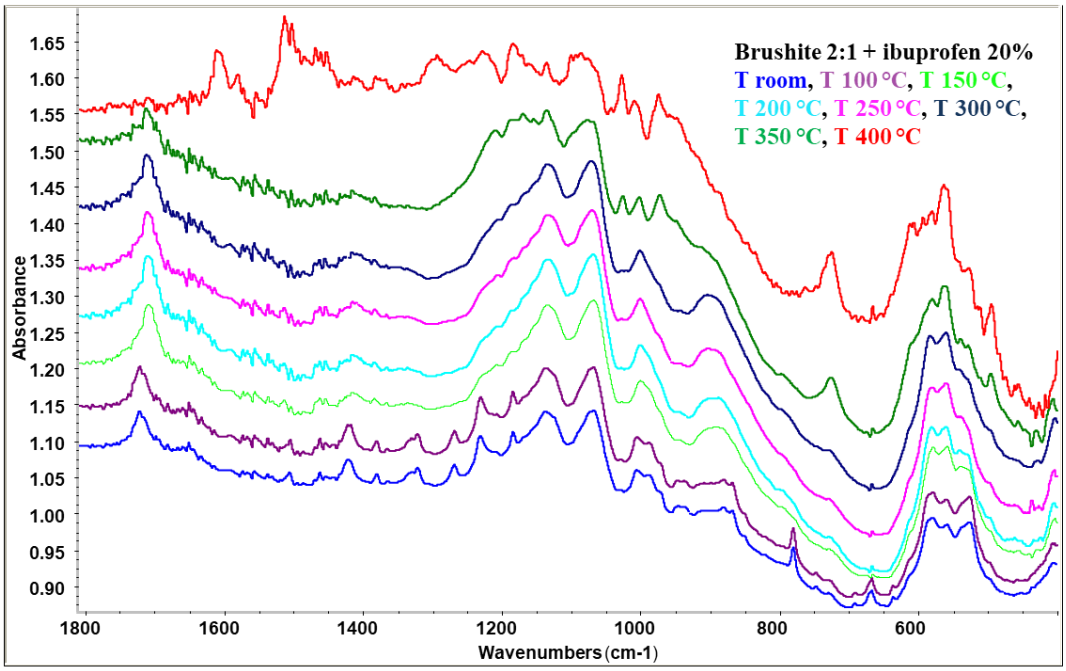

Figure 31. *FT-IR Spectra of brushite 2:1 + ibuprofen 20% at different temperatures increasing from the bottom (no common scale).*

Also in this case, the focus was on the frequencies between 400 and 1800 cm^{-1}. Here the carbonyl group (1600-1800 cm^{-1}) remains but the molecule is broken. There is a peak at 1720 cm^{-1}that drops to 1710 cm^{-1}, this is due to electron-withdrawing effect. The bands present at 1295 cm^{-1}, 1465 cm^{-1}, 1510 cm^{-1} and 1610 cm^{-1} represent the organic residue. As with single brushite, the clear change in the spectrum of the sample with brushite + ibuprofen 20% is seen at 350 °C and 400 °C, when the inorganic matrix converts to pyrophosphates while the organic molecules appear to decompose between 1200-1500 cm^{-1} although the carbonyl group (band at almost 1700 cm^{-1}) is still evident up to 350 °C. The results obtained from this analysis are consistent with those of TGA.

3. TGA naproxen and brushite + naproxen

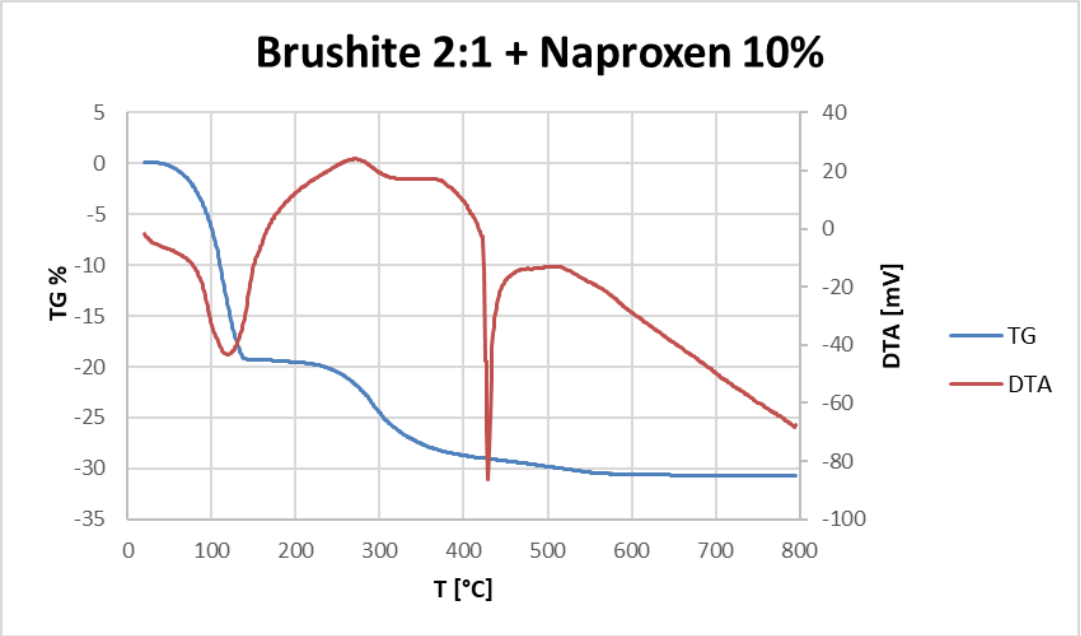

Figure 32. *TGA brushite 2:1 + naproxen 10%.*

Regarding the brushite 2:1 + naproxen 10% sample (108.1 mg), there are the following endothermic peaks (**Figure 32**): 121 °C, 320 °C and 429 °C. In the first case the mass loss is about 19% w/w, in a range between 20 °C and 141 °C, and overall in the other two is 10% w/w, in a range between 211 °C and 505 °C.

Also here, the first peak correspond to the transition from brushite to monetite. The third is probably due to the transformation to calcium pyrophosphate.

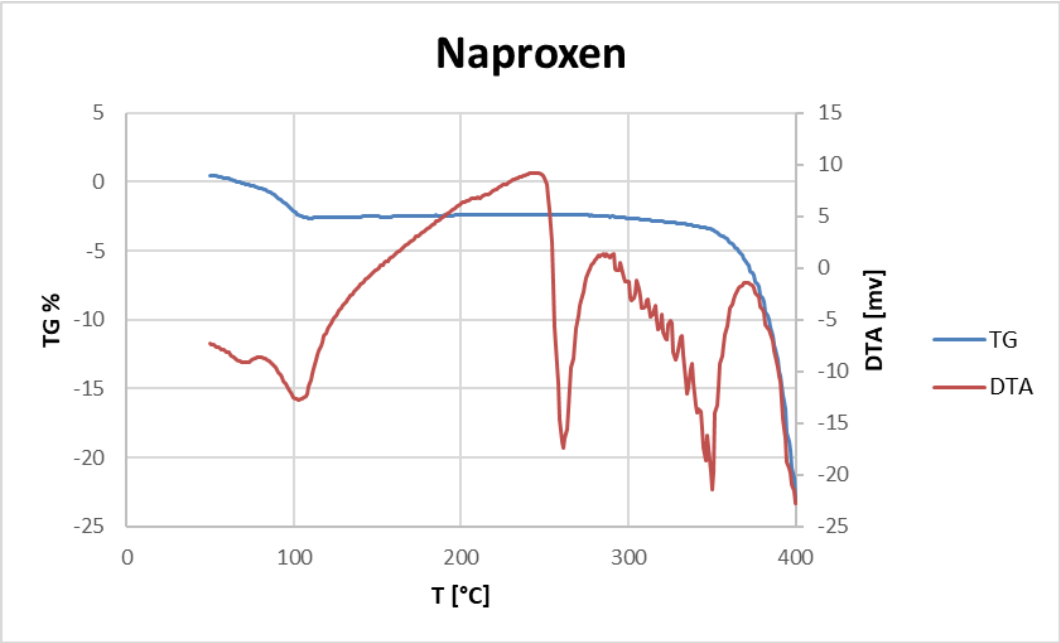

Figure 33. *TGA naproxen.*

Instead the sample of naproxen (78.3 mg) reveals several endothermic peaks (**Figure 33**): 72 °C, 107 °C, 261 °C and several oscillations between 298 °C and 350 °C. Between the first two there is a mass loss of about 22% w/w, in a range between 50 °C and 114 °C, for the third it is minimal and there is again a visible loss from 368 °C.

Up to 400 °C, it can be seen the trend that the sample with brushite also shows in some parts, after that it was noticed that over that temperature, naproxen swells and then begins to burn.

4. IR spectra of brushite, brushite + ibuprofen and brushite + naproxen after TGA

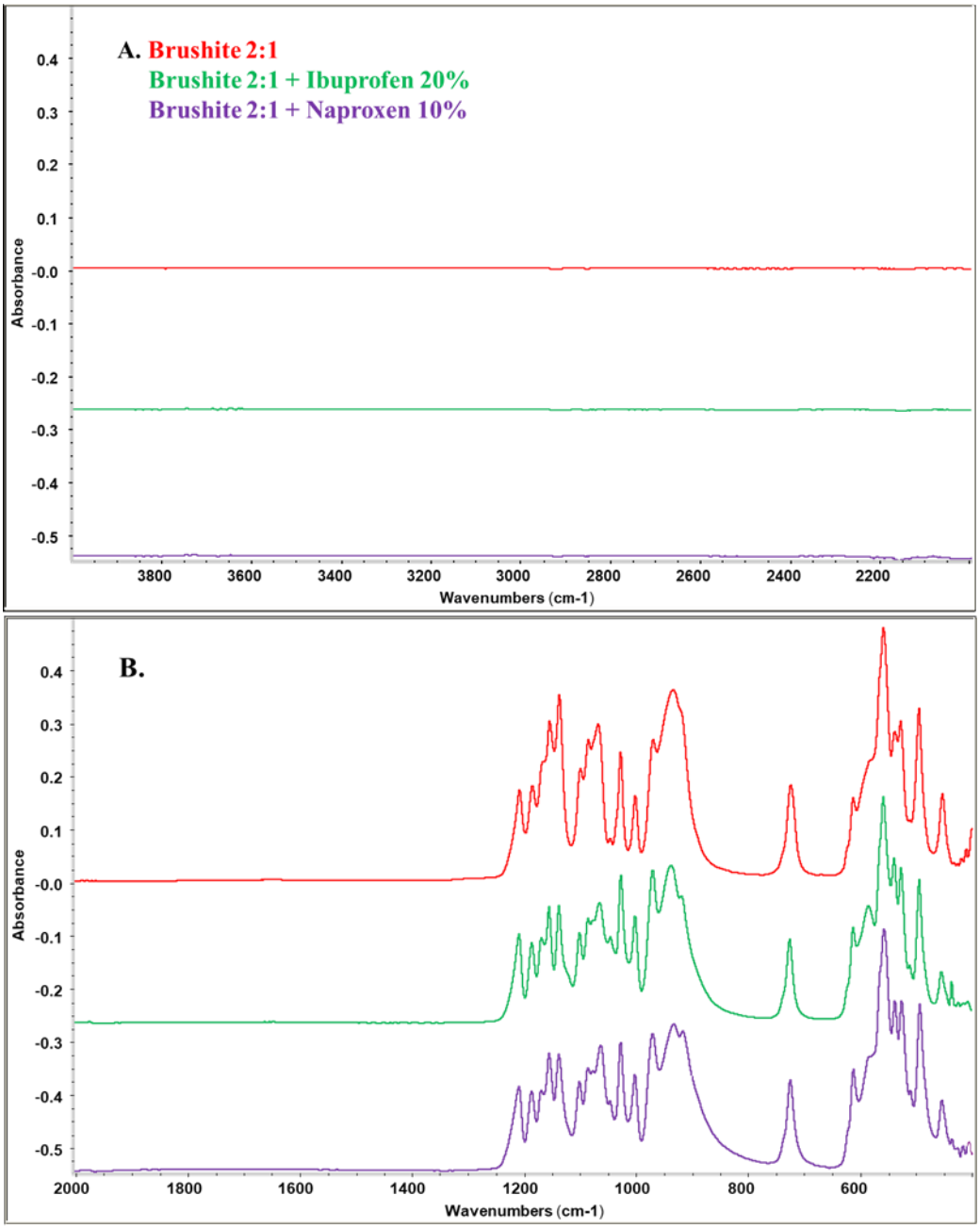

Figure 34. *FT-IR Spectra of brushite 2:1, brushite 2:1 + ibuprofen 20% and brushite 2:1 + naproxen 10% after TGA (no common scale). A) Low frequencies. B) High frequencies.*

After TG analysis of the 2:1 brushite, brushite 2:1 + ibuprofen 20% and brushite 2:1 + naproxen 10% samples (**Figure 34**), IR spectroscopy was also conducted. This allowed to verify the state of the samples after being subjected to high temperatures. After TG, the samples appear to be dehydrated. In figure A it can be seen that the bands related to brushite and monetite are absent. In figure B it is still possible to see the bands

typical of calcium pyrophosphate such as: around 1000-1200 cm^{-1} and 500-600 cm^{-1} [45].

5. TGA gentamicin and brushite + gentamicin

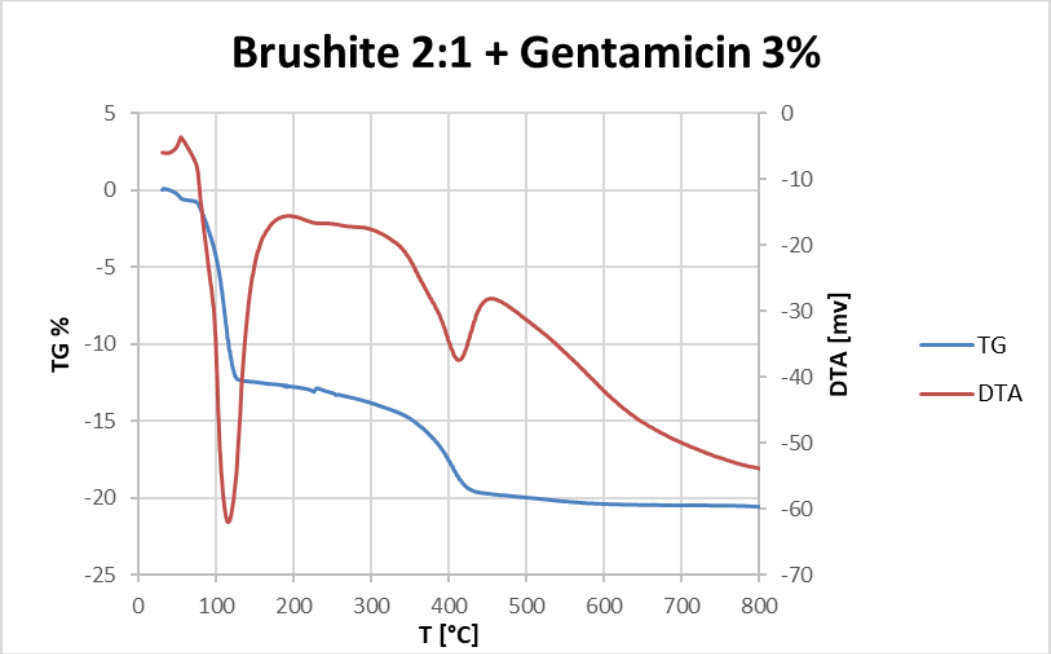

Figure 35. *TGA brushite 2:1 + gentamicin 3%.*

In the case of the brushite + gentamicin 3% sample (117.47 mg), there are two endothermic peaks (**Figure 35**) at 117 °C and 415 °C. In the first case the mass loss is about 12% w/w, in a range between 30 °C and 161 °C. In the second is about 4% w/w, in a range between 359-500 °C.

Also for this sample it can be assumed that the first peak corresponds to the transition of brushite to monetite and the second is that of the transition to calcium pyrophosphate.

Notions from the literature were used for the TGA of gentamicin and the plot can be seen in **Figure 36**.

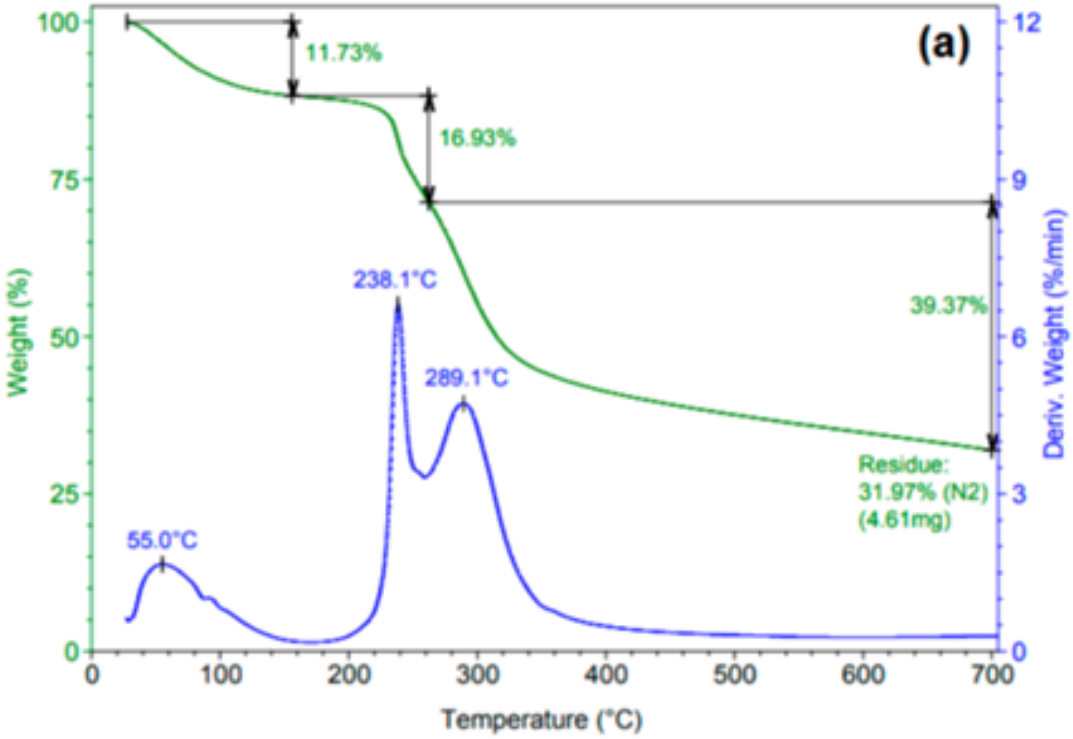

Figure 36. *TGA gentamicin.*

Gentamicin sulfate was also used in this study. It was solubilized in 3% water and 1 ml was analyzed. To determine the effect of temperature on mass loss, these temperature ranges were studied: 40-156 °C, 156-262 °C and 267-700 °C. The beginning of its decomposition starts at about 240 °C. For the first interval there is a weight loss of 11.73 % (Tmax 55 °C), in the second it is 16.93 % (Tmax 293.1 °C) and in the third it is 39.37 % (Tmax 289.1 °C). At 700 °C, the residue is 31.97% [42].

6. DSC brushite, brushite + drugs and drugs

The following are plots of the DSC performed on the samples mentioned in **Table 2**. It provides a more detailed view of how the samples behave at low temperatures and allows for quantitative analysis.

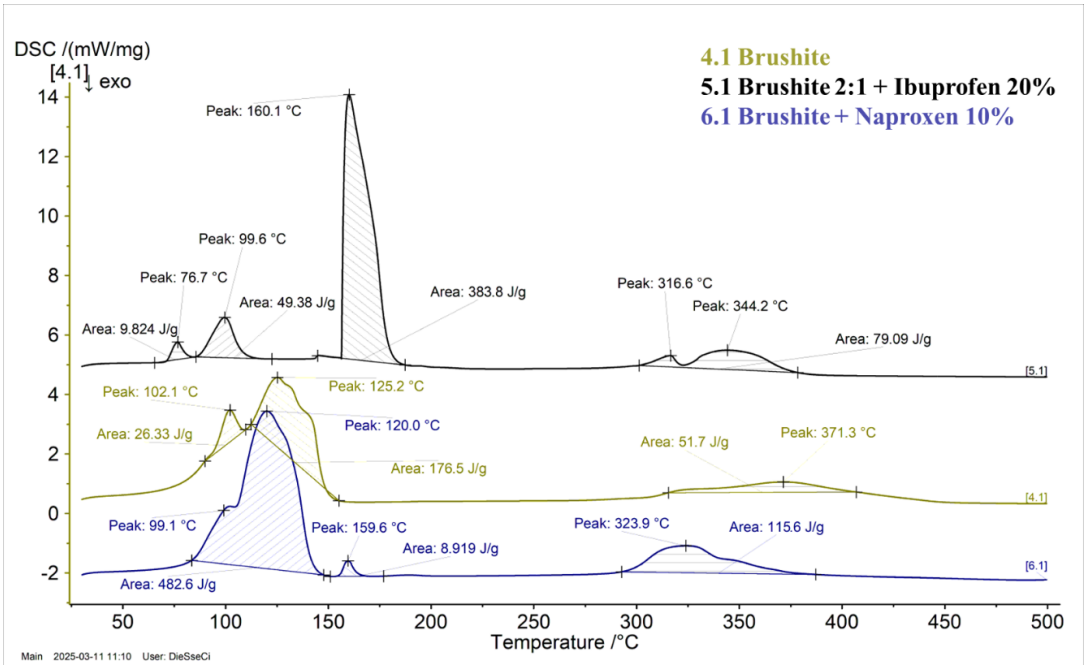

Figure 37. *DSC of brushite 2:1, brushite 2:1 + ibuprofen 20% and brushite + naproxen 10%. They are in common scale but have been shifted.*

The weights of the samples analyzed (**Figure 37**) are as follows:

- 12.87 mg for brushite 2:1.
- 13.65 mg for brushite 2:1 + ibuprofen 20%.
- 12.81 mg for brushite 2:1 + naproxen 10%.

Brushite has three endothermic peaks: 102.1 °C, 125.2 °C, 371.3 °C. The first two represent humidity loss, there are two just for the presence of different pores in the material. The other two are for the loss of crystallization water. The area subtended by the curve represents the ΔH of reaction, for the first peak is 26.33 J/g, for the second is 176.5 J/g and for the third is 51.7 J/g.
Brushite 2:1 + ibuprofen 20% has five endothermic peaks: 76.7 °C, 99.6 °C, 160.1 °C, 316.6 °C and 344.2 °C . With a ΔH respectively of: 9.824 J/g, 49.38 J/g, 383.8 J/g and for the last two collectively of 79.09 J/g.
While for brushite 2:1 + naproxen 10 % has four endothermic peaks: 99.1 °C, 120 °C, 159.6 °C and 323.9 °C. With a ΔH respectively of: 482.6 J/g for the first two combined, 8.919 J/g and 115.6 J/g.
For both drugs around 100 °C there is humidity loss and that of crystallization water is from 300 °C.

It can be seen that interaction with drugs causes some peaks to change, which are found to be shifted to higher temperatures. With ibuprofen the

change of the first peaks is evident and thus there was a strong interaction, also due to the higher percentage of drug than for naproxen.

Pure drugs were also analyzed.

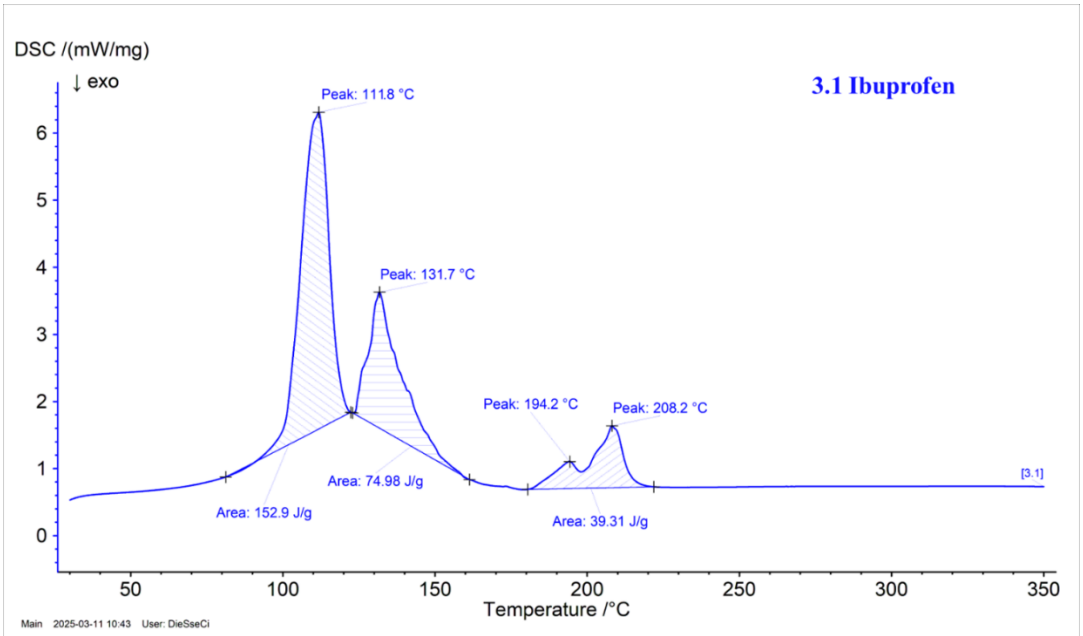

Figure 38. *DSC ibuprofen.*

The weight of the samples of ibuprofen analyzed is 12.80 mg (**Figure 38**). It has four peaks: 111.8 °C, 131.7 °C, 194.2 °C and 208.2 °C. With a ΔH respectively of: 152.9 J/g, 74.98 J/g and 39.31 J/g for the last two.

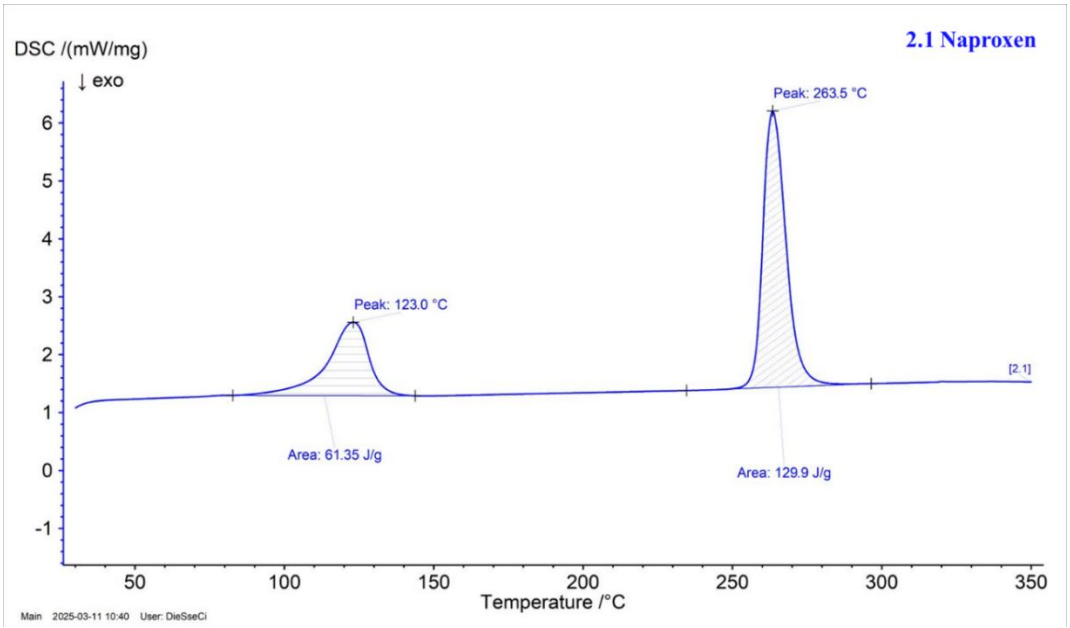

Figure 39. *DSC naproxen.*

The weight of the samples of naproxen analyzed is 11.10 mg (**Figure 39**). Naproxen has few endothermic two endothermic peaks: 123 °C and 263.5 °C. With a ΔH respectively of: 61.35 J/g and 129,9 J/g.

For both drugs, the change of some peaks compared with brushite samples can be verified. This occurs because, as mentioned for TGA, the drug binds to the matrix and causes endothermic peak changes.

Following the same procedures, the sample with the antibiotic was also analyzed.

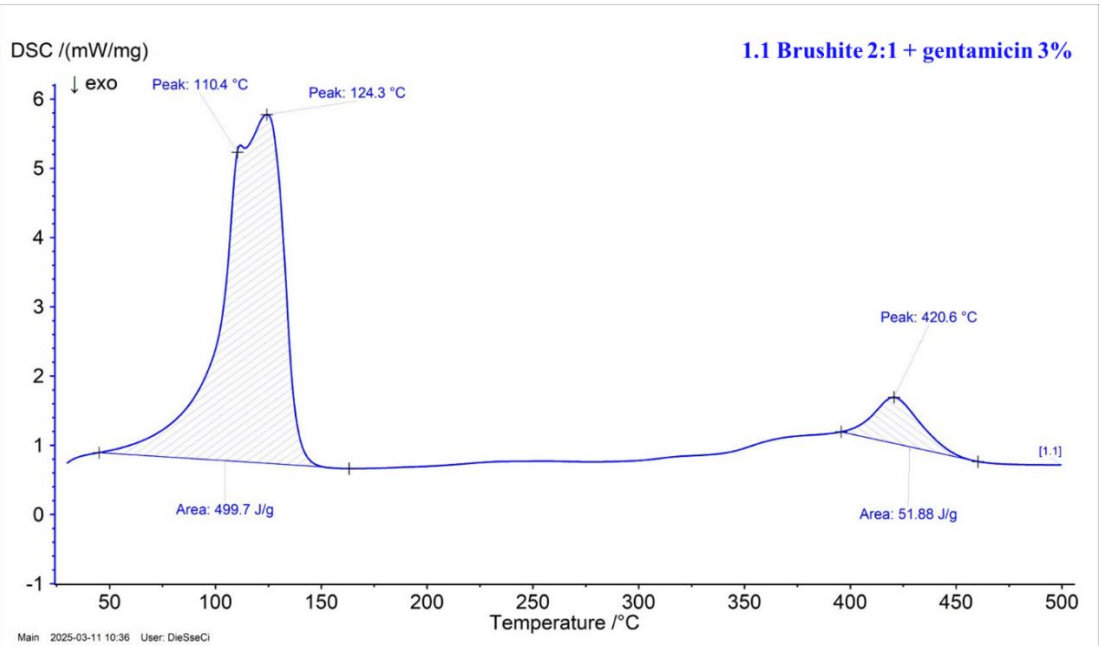

Figure 40. *DSC brushite 2:1 + gentamicin 3%.*

The weight of the sample of brushite 2:1 + gentamicin 3% is 14.59 mg (**Figure 40**). It has three endothermic peaks: 110.4 °C, 124.3 °C and 420.6 °C. With a ΔH respectively of: 499.7 J/g for the first two and 51.88 J/g. Also here around 100 °C there is humidity loss and that of crystallization water is from 300 °C. The low percentage of gentamicin does not influence cause large changes compared to single brushite, it only slightly shifts the peaks.

From the studies found in the literature, it is reported a wide range of melting temperature depending on gentamicin structure. They confirm that the melting point of gentamicin sulfate is about 250 °C [46].

3.4 Study of ibuprofen release

In order to have a correlation of the data, pure ibuprofen samples were analyzed with the spectrophotometer. Then a calibration curve was obtained both before freezing and after. PBS did not interfere with the analysis. The plots for the dilution of the ibuprofen samples can be seen in **Figure 41**, **Figure 42** and **Figure 43**.

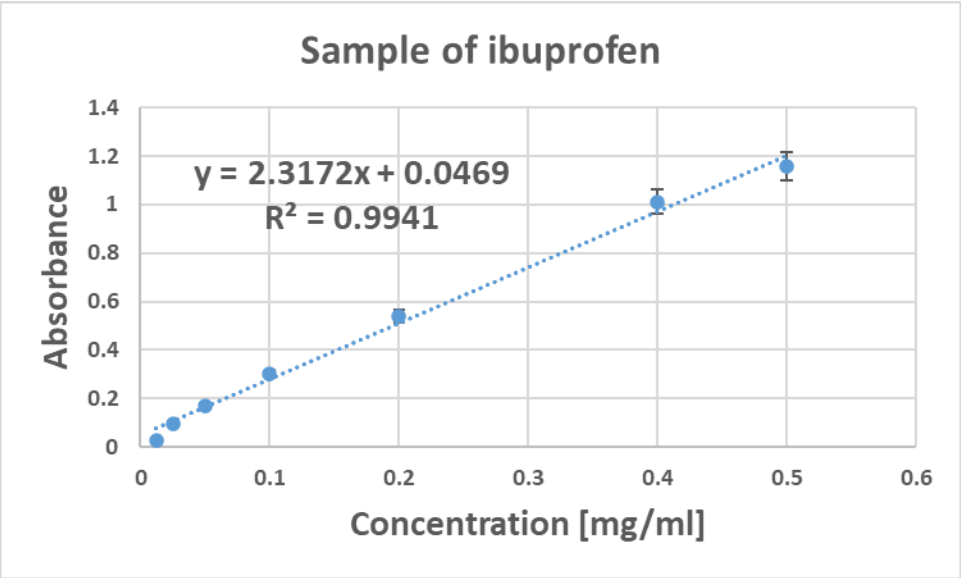

Figure 41. *Calibration curve for ibuprofen before freezing.*

A correlation between the absorbance of ibuprofen and its concentration is obtained from the plot and is represented by the equations in the figure. Where y = absorbance and x = concentration.

This procedure was repeated even after freezing and it was done as many times as brushite and brushite release samples with ibuprofen were also analyzed. This has been done to verify that there were no negative effects of freezing and thawing.

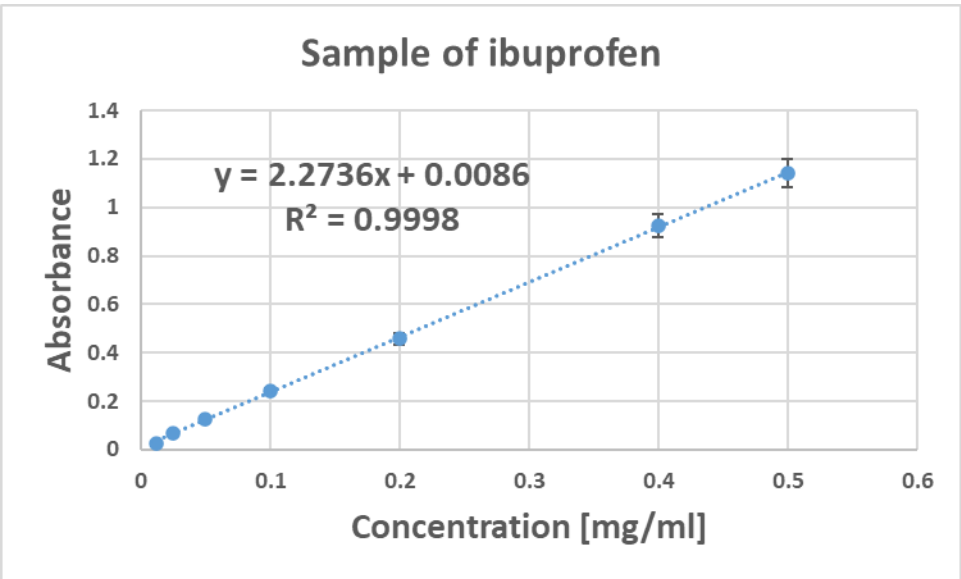

Figure 42. *Calibration curve for ibuprofen after freezing (5 days).*

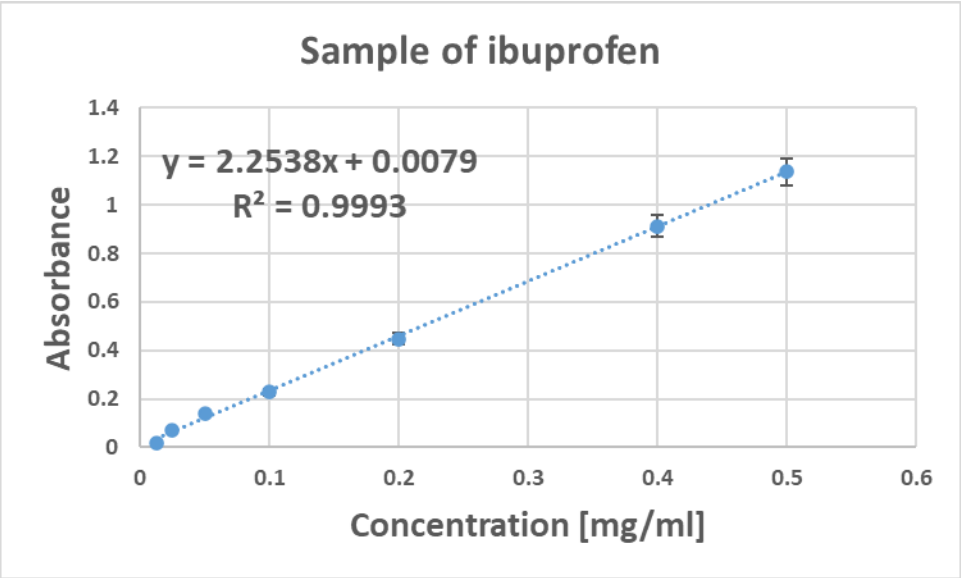

Figure 43. *Calibration curve for ibuprofen after freezing (9 days).*

This allows to see how freezing does not condition the samples since the two graphs are very similar.

Later, the release of brushite 2:1 and brushite 2:1 + ibuprofen 20 % samples taken within one week was analyzed.

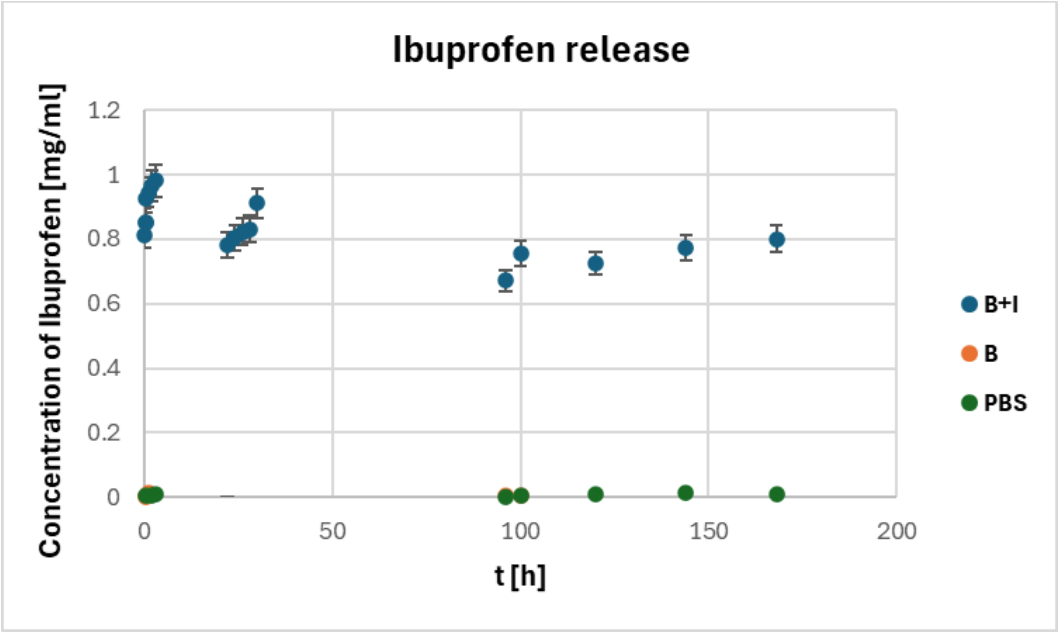

Figure 44. *Ibuprofen release in time. Where B+I =brushite 2:1 + ibuprofen 20%, B=brushite 2:1 and PBS.*

Three moments can be highlighted in **Figure 44**:

- Initial behavior within 3 hours. Ibuprofen release increases relatively smoothly with values ranging from about 0.8 mg/ml up to 1 mg/ml. This is consistent with a rapid release of ibuprofen at the beginning, also considering that 20% w/w was used in the preparation.
- Behavior between 22 and 30 hours. The released concentration decreased from the initial interval.
- Final behavior between 96 and 168 hours. There is further release but the values seem more stable. If the release was completed in the first few hours, it could be that the concentration is reaching a system equilibrium.

Therefore the ibuprofen release curve shows that during the time interval considered, the concentration tends to drop to about 0.8 mg/ml. Brushite and PBS samples do not release anything.

Considering the immediate release, this result should be evaluated according to the required use of the ibuprofen-loaded bone cement (chapter **1.7 Bone cements and drugs**). The interaction between brushite and ibuprofen affects the pharmacokinetics of the pure drug [47]. In fact, in the first three hours, the ibuprofen present on the surface of the sample dissolved in the liquid and it was released, for this reason there has been a burst release. Instead, as hours pass, the system settles and the release becomes almost continuous over time. For future medical applications, it should be considered whether an initial rapid release is necessary over time, or if encapsulating the ibuprofen before binding it to the bone cement matrix is required to achieve a more gradual release of the drug.

4. Conclusions

In this thesis, the potential of brushite-based bone cements also combined with a chemical retardant, sodium citrate, or loaded with drugs was studied. In particular, the effect of two anti-inflammatories agents: ibuprofen and naproxen and an antibiotic: gentamicin, was analyzed. All the required samples were successfully obtained.

During sample preparation, better workability was found for brushite 3:1 but a true retardant effect was obtained with 0.5 molar sodium citrate. The latter also contributed to the lowering of the reaction temperature. As for drugs, the only one that achieved a setting retardant effect was ibuprofen, possibly due to the chelation effect of the calcium ions by the carboxylic group.

FT-IR analysis made it possible to identify the various bands typical of brushite, retardant and drugs, with comparisons found in the literature. This made it possible to verify that the interaction between drugs and brushite causes the changes of some bands and the appearance of others. An example is the band characterizing COOH group for samples with ibuprofen and naproxen whose appearance is likely due to the pH decreasing during the formation of brushite which leads to the formation of free the acidic form of the drugs. The percentage of gentamicin in the composite sample is too low to evidence significant changes in the spectrum.

Also the thermal analysis studied by TGA and DSC, evidences brushite-drug interactions in the case of ibuprofen and naproxen. The interaction of brushite with ibuprofen causes the shift of some endothermic peaks to higher temperatures. This effect with naproxen it is less obvious because of a lower percentage of the drug. Again, the percentage of gentamicin is too low to show strong changes. In the case of brushite 2:1 and brushite 2:1 + ibuprofen 20% w/w thermal analysis was done at increasing temperature followed by IR spectroscopy. This study evidenced changes in the spectra that confirmed the formation of pyrophosphate at high temperatures, especially at 350 °C and 400 °C.

In the end, the release of ibuprofen over time was studied by taking several samples over one week. This showed that the ibuprofen release of the brushite 2:1 + ibuprofen 20% sample is most intense in the first three hours and tends to decrease over a week. The interaction between the two affected the pharmacokinetics of the drug itself. This result should be considered in relation to future medical use.

All of these analyses provided a better understanding of the potential that drug-loaded bone cements present. Looking forward, this still represents an area that needs further study but may prove essential for treating some typical bone diseases.

5. Acknowledgements

I would like to express my gratitude to Professor Elisabetta Finocchio, Professor Alberto Lagazzo and Professor Pier Francesco Ferrari for making this thesis possible and for their guidance throughout the research process.

I would also like to thank everyone at the Materials Engineering Laboratory and at the CBA of San Martino Hospital for their support in completing my work and for their collaborative efforts.

A heartfelt thank you goes to my family and friends for their support throughout my entire academic journey. Especially my parents, who helped me during the most difficult times. I owe it to them that I never gave up.

6. **References**

[1] Le B.Q., Nurcombe V., Cool S.M., Van Blitterswijk C.A., De Boer J., LaPointe V.L.S. "The Components of Bone and What They Can Teach Us about Regeneration." *Materials*, 2018: 11(1):14. https://doi.org/10.3390/ma11010014.

[2] Arcuri C., Artico M., Bertagnolo V., Cataldi A., Conconi M.T., Falconi M., Gobbi P., Grimaldi P., Maxia C., Onori P., Pirino A., Santoro G., Sassoli C., Sferra R., Sisto M., Soldani P., Szychlinska M.A., Toni R., Turci M., Zarcone D. *Anatomia Umana - Elementi - con isituzioni di Istologia.* p. 50-52: edi-ermes, 2019.

[3] Florencio-Silva R., Sasso G.R., Sasso-Cerri E., Simões MJ., Cerri PS. "Biology of Bone Tissue: Structure, Function, and Factors That Influence Bone Cells." *Biomed Res Int.*, 2015: 421746: 10.1155/2015/421746.

[4] Lumen learning. *Types of Bone - Biology for Majors II.* https://courses.lumenlearning.com/wm-biology2/chapter/types-of-bone/.

[5] Medical news today. *What to know about bone diseases.* Last login: 16/03/2025., 2023. https://www.medicalnewstoday.com/articles/bone-diseases.

[6] Hu B., Zhang Y., Zhang G., Li Z., Jing Y., Yao J., Sun S., "Research progress of bone-targeted drug delivery system on metastatic bone tumors.", *Journal of Controlled Release, Volume 350*, 2022: p. 377-388, https://doi.org/10.1016/j.jconrel.2022.08.034.

[7] Pylostomou A., Demir Ö., Loca D. "Calcium phosphate bone cements as local drug delivery systems for bone cancer treatment.", *Biomater Adv*, 2023: 148:213367. 10.1016/j.bioadv.2023.213367.

[8] Huang K.Y., Chen Y.W., Liang T.Y., Lai M.H., Tsai J.C, Shyong Y., "Evaluation of calcium phosphate-zoledronic acid microparticles as a localized delivery system on bone defect: An in vivo study.". *Journal of Drug Delivery Science and Technology*, 2023: 91. 105260. 10.1016/j.jddst.2023.105260.

[9] Demir-Oğuz Ö., Boccaccini A.R., Loca D. "Injectable bone cements: What benefits the combination of calcium phosphates and bioactive glasses could bring?" *Bioact Mater*, 2022: 19:217-236. 10.1016/j.bioactmat.2022.04.007.

[10] O'Dowd-Booth C., White J., Smitham P., Khan W., Marsh D., "Bone Cement: Perioperative Issues, Orthopaedic Applications and Future Developments.", *Journal of perioperative practice*, 2011: 21. 304-8. 10.1177/175045891102100902.

[11] Sivakumar P.M., Yetisgin A.A., Demir E., Sahin S.B., Cetinel S. "Polysaccharide-bioceramic composites for bone tissue engineering: A review.", *Int J Biol Macromol* , 2023: 1;250:126237. 10.1016/j.ijbiomac.2023.126237.

[12] Liu H., Li P., Tang Z., Liu H., Zhang R., Ge J., Yang H., Ni X., Lin X., Yang L. "Study on injectable silver-incorporated calcium phosphate composite with enhanced antibacterial and biomechanical properties for fighting bone cement-associated infections." *Colloids Surf B Biointerfaces*, 2023: 227:113382. 10.1016/j.colsurfb.2023.113382.

[13] Zhang J., Liu W., Schnitzler V., Tancret F., Bouler J.M. "Calcium phosphate cements for bone substitution: chemistry, handling and mechanical properties.", *Acta Biomater*, 2014: 10(3):1035-49. 10.1016/j.actbio.2013.11.001.

[14] Ginebra M.P., Espanol M., Montufar E.B., Perez R.A., Mestres G. "New processing approaches in calcium phosphate cements and their applications in regenerative medicine.", *Acta Biomater*, 2010: 10.1016/j.actbio.2010.01.036.

[15] Richter R.F., Vater C., Korn M., Ahlfeld T., Rauner M., Pradel W., Stadlinger B., Gelinsky M., Lode A., Korn P. "Treatment of critical bone defects using calcium phosphate cement and mesoporous bioactive glass providing spatiotemporal drug delivery.", *Bioact Mater*, 2023: 28:402-419. 10.1016/j.bioactmat.2023.06.001.

[16] Lagazzo A., Barberis F., Carbone C., Ramis G., Finocchio E. "Molecular level interactions in brushite-aminoacids composites.", *Materials Science and Engineering: C*, 2017: P. 721-727, https://doi.org/10.1016/j.msec.2016.09.030.

[17] Sun H., Zhang C., Zhang B., Song P., Xu X., Gui X., Chen X., Gonggong L., Li X., Liang J., Sun J., Jiang Q., Zhou C., Fan Y., Zhou X., Zhang X., "3D printed calcium phosphate scaffolds with controlled release of osteogenic drugs for bone regeneration.", *Chemical Engineering Journal*, 2021: 427. 130961. 10.1016/j.cej.2021.130961.

[18] Darghiasi S.F., Farazin A., Ghazali H.S. "Design of bone scaffolds with calcium phosphate and its derivatives by 3D printing: A review.", *J Mech Behav Biomed Mater*, 2024: 151:106391. 10.1016/j.jmbbm.2024.106391.

[19] Hofmann M.P., Mohammed A.R., Perrie Y., Gbureck U., Barralet J.E. "High-strength resorbable brushite bone cement with controlled drug-releasing capabilities.", *Acta Biomater*, 2009: 5(1):43-9. 10.1016/j.actbio.2008.08.005.

[20] Hurle K., Oliveira J.M., Reis R.L., Pina S., Goetz-Neunhoeffer F. "Ion-doped Brushite Cements for Bone Regeneration.", *Acta Biomater*, 2021: 123:51-71. 10.1016/j.actbio.2021.01.004.

[21] Sugama T. "Citric acid as a set retarder for calcium aluminate phosphate cements.", *Advances in Cement Research - ADV CEM RES*, 2006: 18. 47-57. 10.1680/adcr.2006.18.2.47.

[22] Gbureck U., Barralet J.E., Spatz K., Grover L.M., Thull R. "Ionic modification of calcium phosphate cement viscosity. Part I: hypodermic injection and strength improvement of apatite cement.", *Biomaterials*, 2004: 25(11):2187-95. 10.1016/j.biomaterials.2003.08.066.

[23] Dorozhkin S.V., "Calcium orthophosphate cements for biomedical application.", *J Mater Sci.*, 2008: 43:3028–3057. 10.1007/s10853-008-2527-z.

[24] *Wikipedia. Tecnologia odontotecnica.* Last login: 16/03/2025. https://it.wikipedia.org/wiki/Tecnologia_odontotecnica?utm_source=.

[25] Ginebra M.P., Traykova T., Planell J.A. "Calcium phosphate cements as bone drug delivery systems: a review.", *J Control Release*, 2006: 113(2):102-10. 10.1016/j.jconrel.2006.04.007.

[26] Soares F., Ribeiro N., Baião A., Torres P., Sarmento B., Olhero S. "Sustained drug release from sintering-free calcium phosphate-based scaffolds." *Journal of Drug Delivery Science and Technology*, 2023: 88. 104906. 10.1016/j.jddst.2023.104906.

[27] *Cemex Genta LV. Tecres. Last login: 16/03/2025.* https://www.tecres.it/dettagli-prodotto/cemex-genta-lv-1?utm_source=.

[28] Tamimi F., Sheikh Z., Barralet J. "Dicalcium phosphate cements: brushite and monetite." *Acta Biomater*, 2012: 8(2):474-87. 10.1016/j.actbio.2011.08.005.

[29] *Sigma-Aldrich - Ibuprofen sodium salt. Last login: 16/03/2025.* https://www.sigmaaldrich.com/IT/it/search/ibuprofen-sodium-salt?focus=products&gclid=EAIaIQobChMIg721joTaiwMVmpKDBx12LBldEAAYASAAEgKrVvD_BwE&page=1&perpage=30&sort=relevance&term=ibuprofen%20sodium%20salt&type=product_name&utm_campaign=20856404117&utm_con.

[30] *Sigma-Aldrich - Naproxen sodium. Last login: 16/03/2025.* https://www.sigmaaldrich.com/IT/it/substance/naproxensodium2522426159342.

[31] *Sigma-Aldrich - Gentamicin sulfate salt. Last login: 16/03/2025.* https://www.sigmaaldrich.com/IT/it/substance/gentamicinsulfate123451405410.

[32] *National Center for Biotechnology Information. PubChem. - Gentamicin C1 sulfate. Last login: 16/03/2025.* https://pubchem.ncbi.nlm.nih.gov/compound/gentamicin-C1-sulfate.

[33] Munajad A., Subroto C., & Suwarno. "Fourier Transform Infrared (FTIR) Spectroscopy Analysis of Transformer Paper in Mineral Oil-Paper Composite Insulation under Accelerated Thermal Aging.", *Energies,*, 2018: 11(2), 364. https://doi.org/10.3390/en11020364 .

[34] *Mettler Toledo. Attenuated total reflectance (ATR) spectroscopy. Last login: 16/03/2025.* https://www.mt.com/it/it/home/applications/L1_AutoChem_Applications/ftir-spectroscopy/attenuated-total-reflectance-atr.html.

[35] *Tecan. Multimode plate reader. Last login: 16/03/2025.* https://lifesciences.tecan.it/multimode-plate-reader.

[36] *Technology Networks. UV-Vis spectroscopy: Principle, strengths, limitations, and applications. Last login: 16/03/2025.* https://www.technologynetworks.com/analysis/articles/uv-vis-spectroscopy-principle-strengths-and-limitations-and-applications-349865.

[37] Hirsch A., Azuri I., Addadi L., Weiner S., Yang K., Curtarolo S., Kronik L. "Infrared Absorption Spectrum of Brushite from First Principles.", *Chemistry of Materials*, 2014: 26 (9), 2934-2942. 10.1021/cm500650t.

[38] Mevellec J.Y., Quillard S., Deniard P., Mekmene O., Gaucheron F., et al. "Polarized infrared reflectance spectra of brushite (CaHPO4 center dot 2H(2)O) crystal investigation.", *Spectrochimica Acta Part A: Molecular and Biomolecular Spectroscopy [1994-..]*, 2013: 111, pp.7. 10.1016/j.saa.2013.03.047.

[39] Ravaglioli A., Krajewski A. "Ceramics, cells, and tissues : surface-reactive biomaterials as scaffolds and coatings, interactions with cells and tissues.", *Seminar and Meeting on Ceramics Cells and Tissues (12th 2009 Faenza Italy).* 310-311.

[40] Jubert A., Legarto M.L., Massa N.E., López Tévez L., Okulik N.B. "Vibrational and theoretical studies of non-steroidal anti-inflammatory drugs Ibuprofen [2-(4-isobutylphenyl)propionic acid]; Naproxen [6-methoxy-α-methyl-2-naphthalene acetic acid] and Tolmetin acids [1-methyl-5-(4-methylbenzoyl)-1H-pyrrole-2-acetic acid]." *Journal of Molecular Structure*, 2006: Volume 783, Issues 1–3. https://doi.org/10.1016/j.molstruc.2005.08.018.

[41] Dabiri SMH., Lagazzo A., Barberis F., Shayganpour A., Finocchio E., Pastorino L. "New in-situ synthetized hydrogel composite based on alginate and brushite as a potential pH sensitive drug delivery system", *Carbohydr Polym*, 2017: 177:324-333. 10.1016/j.carbpol.2017.08.046.

[42] Purcar V., Rădiţoiu V., Nichita C., Bălan A., Rădiţoiu A., Căprărescu S., Raduly FM., Manea R., Şomoghi R., Nicolae CA., Raut I., Jecu L. "Preparation and Characterization of Silica Nanoparticles and of Silica-Gentamicin Nanostructured Solution Obtained by Microwave-Assisted Synthesis.", *Materials (Basel)*, 2021: 14(8):2086. 10.3390/ma14082086.

[43] Arakkal A., Paramban S., Sailaja G. "Natural rubber latex films with effective growth inhibition against S. aureus via surface conjugated gentamicin." *Journal of Bioactive and Compatible Polymers*, 2023: 38. 088391152311538. 10.1177/08839115231153823.

[44] Ramukutty S., Ramachandran E." Reaction Rate Models for the Thermal Decomposition of Ibuprofen Crystals.", *Journal of Crystallization Process and Technology*, 2014: Vol.4 No.2. 10.4236/jcpt.2014.42010.

[45] Gras P., Rey C, Marsan O., Sarda S., Combes C. "Synthesis and Characterisation of Hydrated Calcium Pyrophosphate Phases of Biological Interest.", *European Journal of Inorganic Chemistry*, 2013: p.5886-5895. 10.1002/ejic.201300955.

[46] Kenechukwu F., Mumuni M., Nnamani P., Attama A. "Solid lipid micro-dispersions (SLMs) based on PEGylated solidified reverse micellar solutions (SRMS): A novel carrier system for gentamicin.", *Drug Delivery.*, 2014: 10.3109/10717544.2014.900152.

[47] Tillement J.P., Tremblay D. "Clinical Pharmacokinetic Criteria for Drug Research." *2007*, 10.1016/B0-08-045044-X/00117-6.